21. DEEP-WATER CONTINENTAL-MARGIN SEDIMENTATION, DSDP LEG 28, ANTARCTICA

David J.W. Piper and Creighton D. Brisco, Departments of Geology and Oceanography
Dalhousie University, Halifax, Nova Scotia, Canada

ABSTRACT

Sites 268, 269, and 274 lie in deep water on the continental margin of Antarctica to the south of Australia. Site 268, on the continental rise of Wilkes Land, consists of a 150-meter-thick sequence dominated by turbidites, overlying a 300-meter-thick mudstone sequence, with many silt laminae believed formed by bottom ("contour") currents. The turbidity currents were generated by slumping of unstable masses of ice-rafted sediment, a resedimented pebbly mud was recovered, and several otherwise well-sorted and well-graded medium sand beds have lutum contents of 25%-50%. The laminae formed by bottom currents can be distinguished from those of turbidity-current origin by their sedimentary structures and their high content of microfossils, similar to those in interbedded muds. Site 269, on the Wilkes Abyssal Plain, is dominantly a silt-clay turbidite sequence. Sedimentary structures are exceptionally well preserved in the silts and show much evidence of synsedimentary deformation. Although on the continental rise off Victoria Land, Site 274 was protected during most of its history from direct sedimentation from the continent by an upslope graben.

The abundance and grain size of ice-rafted debris at these sites, and Sites 267 and 266, to the north of 268, in an area of pelagic sediments, have been studied. Ice-rafting extends back to at least the lower Miocene in both the Wilkes Land and Ross Sea sectors of Antarctica. Tentative interpretations of the type of ice cover in Antarctica since that time can be made.

At Site 274, ice-rafted sediment appears to derive mainly from Marie Byrd Land, but fine sediment and turbidites appear dominated by a local Victoria Land source. Substantial exposure of the Beacon Group from beneath the Victoria Land basalts probably first occurred in the late Miocene. The petrology of detrital materials at Site 269 is similar and somewhat intermediate to that at Site 268. Crystalline igneous and metamorphic rocks dominate the source area for Site 268, but in post-Miocene sediments there is evidence of significant amounts of Beacon-type detritus.

Dark micronodules of fine-sand size are common at several horizons. Most of these are similar in composition to manganese macronodules and pebble coatings found at Sites 274 and 267. A few are dominantly of iron oxide and clay and contain virtually no manganese. No close correlation appears between micronodules and bottom current activity.

Porcellanous cherts are found in Miocene and Oligocene sediments at Sites 268, 269, 272, and 274. They are formed by the diagenetic growth of disordered cristobalite in mudstones containing biogenic silica. The variety of colors and bedding structures in the mudstones are also found in corresponding cherts. Growth of cristobalite appears to precede pronounced lithification. The source of silica is believed to be finely divided diatom debris but there is no unequivocal evidence for this. Larger diatom and Radiolarian skeletons are found in the cherts and appear to be uncorroded.

INTRODUCTION

Leg 28 of the Deep Sea Drilling Project drilled through thick continental margin sediments in the Australian-New Zealand sector of Antarctica at three sites (Figure 1). Sites 268 and 274 are located on the continental rise; Site 269, on the Wilkes Abyssal Plain. Lower Tertiary sediments were penetrated at all sites. Sites 265, 266, and 267 are in pelagic sediments north of Site 268; Sites 270-273 penetrated shelf sediments in the Ross Sea south of Site 274.

There is already much data available from *Eltanin* piston cores in this region (Payne and Conolly, 1972; Fillon, 1972). These cores have been dated by magnetic reversals coupled with paleontologic dating. Our intermittent near-surface recovery and core deformation preclude the use of paleomagnetic stratigraphy; paleontologic dating in our cores is poor.

The sediment sequences are the result of many interacting sedimentation processes. Ice-rafting is of major importance, especially since later Miocene time. Turbidites are found at all three sites, and "hemipelagic" movement of fine sediments down continental slopes probably also occurs. Bottom currents ("contour currents") are important at the continental rise sites. Siliceous microfossils (mostly diatoms) have accumulated at Site 274 since the Eocene, but at Sites 268 and 269, pre-Pliocene sediments also include calcareous microfossils.

CURRENT-DEPOSITED DEEP-WATER SEDIMENTS

Site 268 (Unit 1)

Three sediment types are found in the upper 160 meters at Site 268:

1) diatom ooze, diatom-bearing silty clay, and intermediate lithologies;

2) clay, silty clay, and clayey silt, with laminae of medium silt; and

3) beds of fine sand.

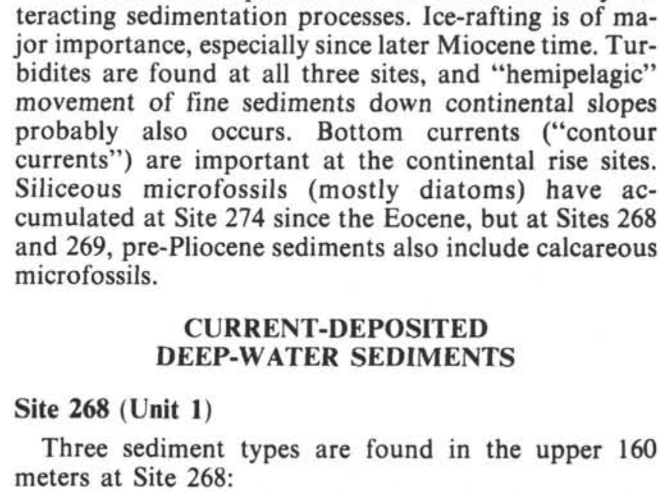

Figure 1. *Location map for Sites 266, 267, 268, 269, 272, and 274. Shows principal Antarctic ice shelves, bathymetry in meters, and subice drainage divides.*

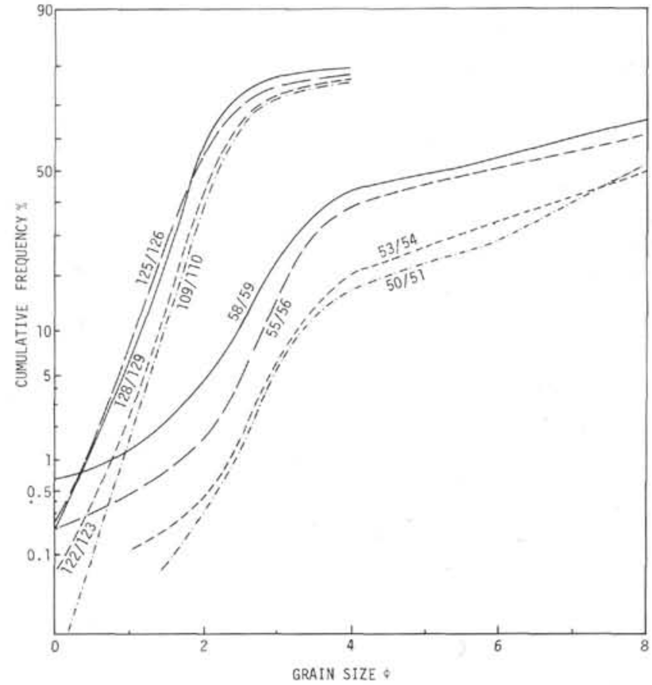

Figure 2. *Grain size analyses of two turbidite sand beds from upper part of Site 268. (a) bed with base at 268-2-2, 130 cm. (b) bed with base at 268-5-2, 59 cm.*

The fine-sand beds are typically 2-20 cm thick, are sharp based, and grade upwards into clayey silt. Two typical beds have been analyzed in detail for grain size (Figure 2). The bed with a base at Sample 268-2-2, 130 cm consists of well-sorted sand, with a mode around 2ϕ, and very little sand in the 3ϕ-4ϕ range. Yet the bed contains 20%-23% lutum (finer than 4ϕ), probably mostly of clay size. Such high lutum contents in graded medium sand beds are most unusual (Kuenen, 1966). A bed with a base at Sample 268-5-2,59 cm has a mode around 3.5ϕ; the sand fraction is poorly sorted, but graded, and the lutum content of the lower part of the bed is around 60%, most of which is of clay size. Spot checks on two other sand beds show high lutum contents.

In the clays and muds, silt laminae are common, both singly and in groups. Diatom contents in these sediments are very low; ice-rafted granules and coarse sand are absent. The laminae are 0.5-2 mm thick, of well-sorted angular quartz and feldspar in the medium- and coarse-silt range. They usually have distinct bases and tops, and are not lenticular. Their appearance is quite different from the laminae in the lower part of the hole, described below. The absence of pelagic biogenic and ice-rafted material in the associated sediment might suggest a high rate of deposition, and hence a turbidite origin; however, there is no direct evidence for this interpretation.

Near the base of Core 1, Section 6, there is a 50-cm-thick bed of pebbly mud, overlain by a 4-cm-thick well-sorted sand bed. The pebbly mud consists of pebbles and granules of crystalline rocks and varicolored clasts of mud of pebble size in a matrix of sandy mud (Figure

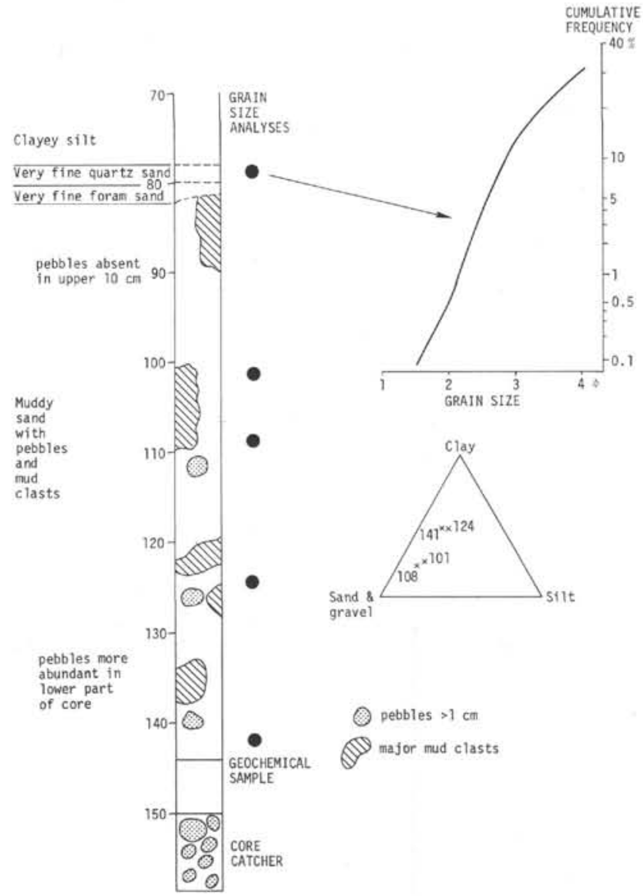

Figure 3. *Sketch section of pebbly mud bed at base of 268-1-6, showing distribution of larger pebbles, and grain size analyses.*

3). Pebbles are much more abundant near the base of the bed.

In the sand bed, well-sorted foraminifera and foraminiferal fragments predominate in the lower part of the bed, while quartz is dominant in the upper part. The foraminifera are entirely *Globigerina pachyderma.* They are also found in other parts of Core 1, and are especially abundant in the pebbly-mud bed. The site generally appears to have been beneath the carbonate compensation depth, and the accumulation of foraminifera presumably represents rapid deposition.

The high *G. pachyderma* content of the sand and the underlying pebbly mud suggests a genetic relationship. Winnowing of the pebbly mud by bottom currents is precluded by the relationship of quartz to foram sand and the lack of coarse sand and granules in the sand bed. The sedimentary sequence is very similar to that described by Kelts and Briegel (1971) from Lake Zurich, produced by a mudflow and a turbidity current apparently generated from it. Resedimentation of shallower water sediments from above the carbonate compensation depth would also explain the high foraminifera content.

Site 268 (Units 2 and 3)

Beds of obvious turbidite origin are absent in the lower two units at Site 268. No sand beds were recovered. The dominant bedding feature is abundant silt laminae (Figures 4, 5). These laminae are often lenticular and frequently do not appear to have sharp bases. Where they occur in diatom- and radiolarian-rich muds, the laminae have concentrations of size-sorted diatoms and Radiolaria.

These laminae appear quite different from those found in turbidite-dominated sequences, for example, Site 269, described below, or DSDP Sites 178-181 in the Gulf of Alaska (Piper, 1973). The site is located on a continental rise. There are thus a priori grounds for considering the laminae to be produced by normal bottom currents or contour currents.

There are no generally accepted criteria in the literature for distinguishing laminae deposited by turbidity and contour currents. Several authors (Field and Pilkey, 1971; Bouma and Hollister, 1973) have erected empirical criteria for distinguishing the two, but they have not satisfactorily demonstrated that their "contourites" are not distal turbidites. Furthermore, some of Hollister's generalizations about turbidites, while they may be true for the area which he investigated, are not applicable to all turbidites.

Turbidity currents differ from contour currents primarily in their much greater suspended sediment load that is necessary to keep them in motion. From this, we may derive the following criteria for distinguishing turbidity-current and contour-current deposits:

1) Deposits with evidence of rapid deposition are probably turbidites. Such evidence would include climbing ripples with no stoss side erosion, animal escape burrows, and dewatering structures.

2) Deposits with evidence of sediment starvation are probably contourites. Such evidence includes isolated ("starved") ripples and perhaps shallow scours not filled with unusually coarse sediments.

3) Evidence of highly turbulent erosion is probably restricted to turbidity currents.

4) The petrographic composition of contourites should follow that of the coarser components of the interbedded sediment; this may also occur in turbidites, but does not appear common.

Presently, no reliable empirical generalizations on textural characteristics appear which allow a distinction of turbidite and contourite laminae, although it may be possible to distinguish thicker beds in this way. Demonstrable turbidite laminae show wide variations in sorting, grading, and grain orientation (Piper, 1972b, 1973). Geographic orientation of a pronounced fabric would probably be a good criterion, but DSDP cores are not oriented.

With so few criteria available, any interpretation of the laminae as contourites must be tentative. The following generalizations can be made about the laminae:

1) They are never thick. Silt lenses are never more than 5 mm thick.

2) Many laminae are lenticular, and thinner laminae are discontinuous.

3) Some laminae have sharp bases and/or tops; in others, the margins are gradual.

4) Where the laminae interbed with muds containing biogenic material, this silt-size material is concentrated

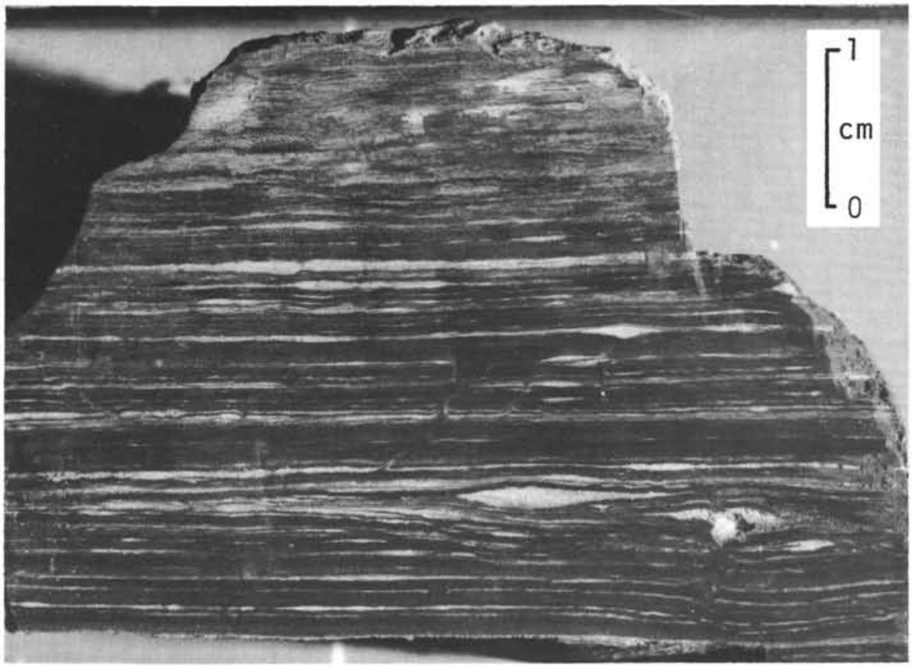

Figure 4. *Probable "contourite" silt laminae, 268-17-3. Note lenticularity of laminae, erosional scours not filled with coarser silt, and slight bioturbation.*

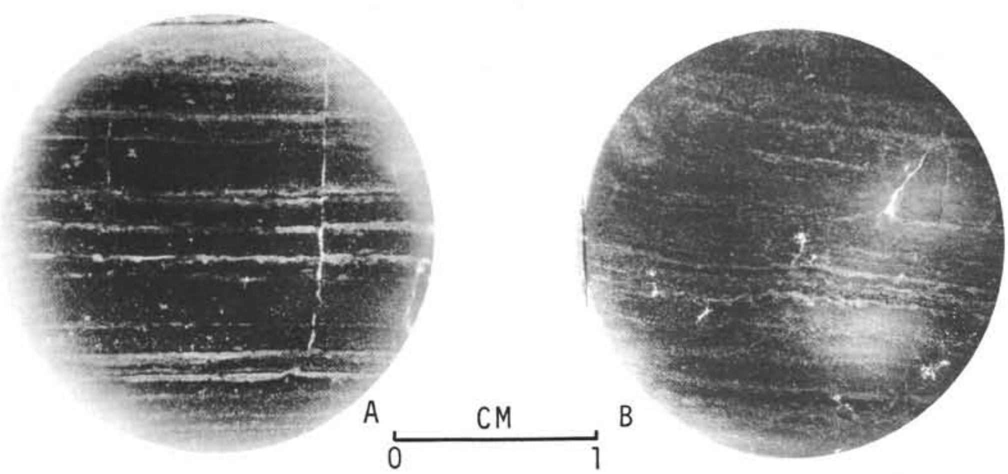

Figure 5. *Probable "contourite" silt laminae in thin sections, Site 268, Cores 10 to 12. (a) 268-10-3, 108-110 cm. (b) 268-10-2, 103-105 cm.*

in the laminae. Laminae may contain up to 25% diatoms and radiolarians in the coarse-silt size range, where the interbedded sediment is a diatom-bearing mud. Where there is little or no biogenic material in the surrounding sediment, the biogenic component of the laminae is correspondingly reduced or absent.

5) Calcium carbonate fossils have not been found in the laminae although occasional coccoliths and foraminifera are found in turbidites from Sites 269 and 274.

6) Demonstrable turbidites from Sites 269 and 274, with a grain size similar to the laminae, contain very few diatom and radiolarian fragments, even though, at least at Site 274, there is an abundance of these microfossils in associated sediments.

7) The laminae appear well sorted in smear slides. The coarsest grains seen reach about 70μ.

8) There is no pronounced grain orientation visible in thin sections cut normal to the bedding plane.

9) No heavy-mineral placers have been seen.

10) Both diatoms and radiolarians often have a dark mineral coating. The nature of this coating has not been determined. It is also found in a few skeletons in the interbedded muds, but the proportion of mineralized fragments in the laminae is much higher. Quartz and other mineral grains do not have the dark coating.

All of the first six points appear more consistent with a contour-current than a turbidity-current origin.

If the interpretation of these laminae as contourites is correct, then the criteria proposed by Bouma and Hollister (1973) for the recognition of contourites must be modified, at least inasmuch as they refer to laminae rather than thicker beds. Specifically, heavy mineral placers are absent, there is no pronounced grain orientation, matrix content is not a basis of distinction from turbidites, and microfossils are commoner than in turbidites.

Site 269

The division of Site 269 into units is rather arbitrary because of the uniformity of the site and the discontinuous coring. It is most simply divided into two parts on the basis of lithification: an upper unlithified part and a lower semilithified part (from which it is possible to make polished slabs and thin sections). Cores in the middle part of the site had very poor recovery, making detailed sedimentology difficult.

Upper Part of 269 (Units 1 and 2)

Diatom oozes and diatomaceous muds dominate the upper part of the section and interbed with sand and silt beds (Figure 6). These beds include (a) Well-sorted very fine sand beds, e.g., Sample 269-1-5, 124-130 cm (Figure 7), 5-30 cm thick with a low lutum content around 10% (cf. Site 268); slight grading visible; sharp base, and sometimes a sharp top. (b) Well-sorted coarse silt beds, e.g., Sample 269-3-3, 14-20 cm (Figure 7), with a sharp base and grading; usually 1-5 cm thick. These appear very similar to those described by Piper (1973) from the Gulf of Alaska. Some beds pass up into alternating laminae of silt and clay. (c) Alternating silt and mud laminae, with the silt laminae occurring in groups in which there is an upward decrease in thickness and grain size of the silt laminae. This is the "graded laminated bed" of Piper (1972b).

Sands are commonest in Core 1, silts are commoner in lower cores. It is seldom possible to make any statements concerning whether mud beds are associated with the silt and sand turbidites. Some such beds certainly grade up into silty mud with few diatoms.

Lower Part of Site 269 (Unit 5)

A detailed study has been made of the lower part of Hole 269A (Sections 6-13), where a sequence of early Miocene or Oligocene claystones and siltstones were intermittently cored. The rocks are semilithified, with water contents in claystones as low as 14%. Recovery, especially in the lower cores, was excellent, with long sections of unbroken core being obtained.

Site 269 is located on the Wilkes Abyssal Plain, about 200 km north of the lower edge of the continental rise. It is probable, from seismic reflection profiles, that the lower part of Hole 269A was located on an abyssal plain in the mid-Tertiary. This interpretation is supported by the similarity of the upper sedimentary sequence of undoubted abyssal plain deposition with the lower part of Hole 269A. The main difference is in the lack of diatoms in the lower part of the hole. Sands are infrequent throughout this hole (Figure 6) and where present appear to be turbidites. A similar paucity of sands has been found on other abyssal plains drilled by DSDP (e.g., Piper, 1973). The lower part of Hole 269A consists of undeformed, fine-grained abyssal plain sediment with sedimentary structures well displayed.

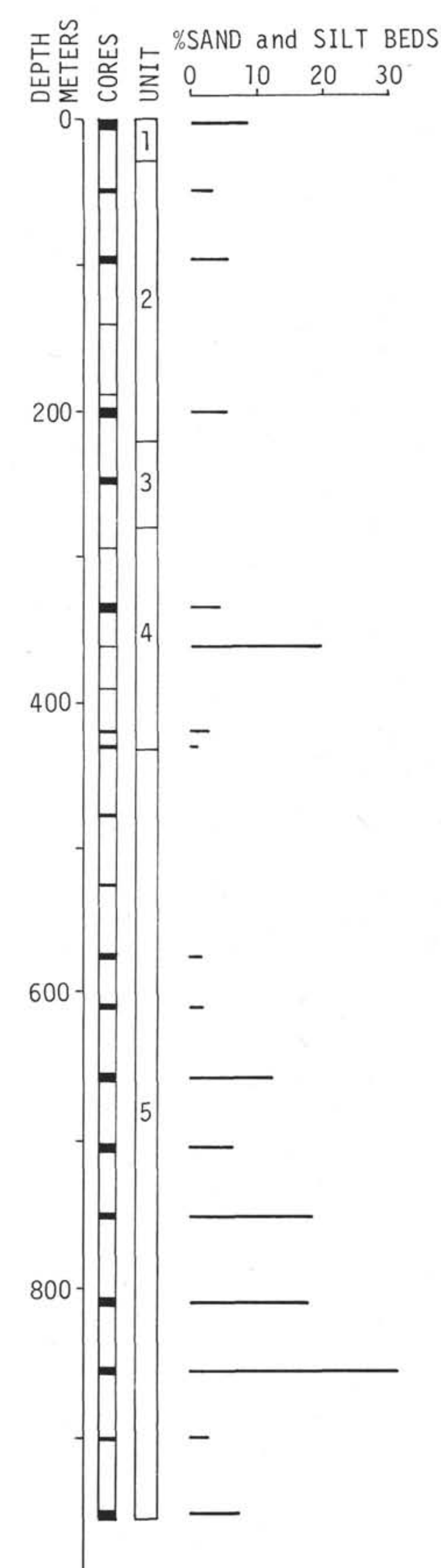

Figure 6. *Distribution of sand and silt beds at Site 269.*

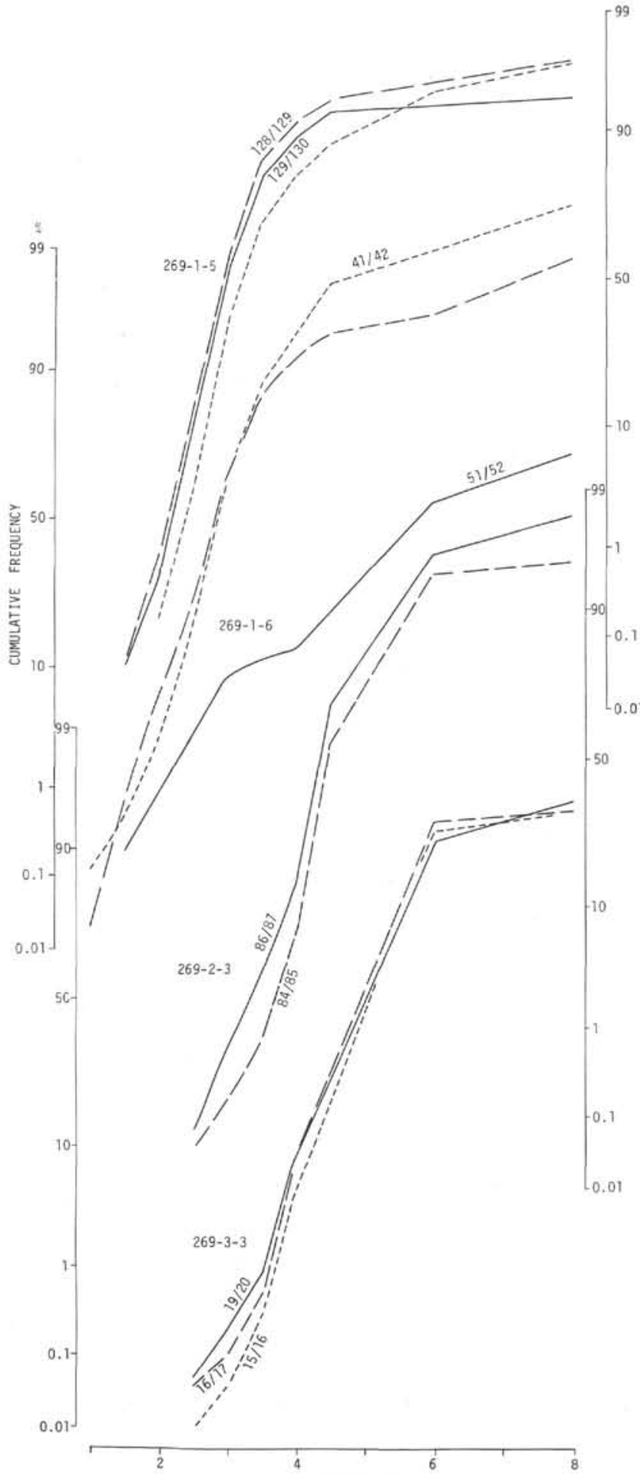

Figure 7. *Grain size analyses of turbidite sand and silt beds from upper part of Site 269, determined by pipette analysis and sieving.*

Cores were split with the band saw and washed clean. Lithologies were logged in detail (centimeter by centimeter) onboard ship. Thin slabs were taken for X-radiography.

Size analysis (Figures 8 and 9) was by conventional sieve and pipette methods. An ultrasonic bath treatment of 1½ hr was necessary to disaggregate samples. Results obtained are consistent with smear slide identifications, but are probably not entirely comparable with samples of unconsolidated sediment. Sandstones with calcium carbonate cement were successfully disaggregated with acetic acid.

The shipboard logging of cores was aimed at objective description. As logging was completed, descriptions were immediately rationalized into about 17 lithologic types. A few core intervals could not be fitted into any of these types. Some core lengths were re-examined to check assignment to lithologic types, but there was no systematic relogging.

From the 17 lithologic types, 10 major facies were recognized (Table 1; Figures 8, 9). These are divided into clay facies and silt facies as follows:

A) **Olive-black claystone:** Sometimes silty claystone. Mottling generally absent. (Facies A2 has very slight

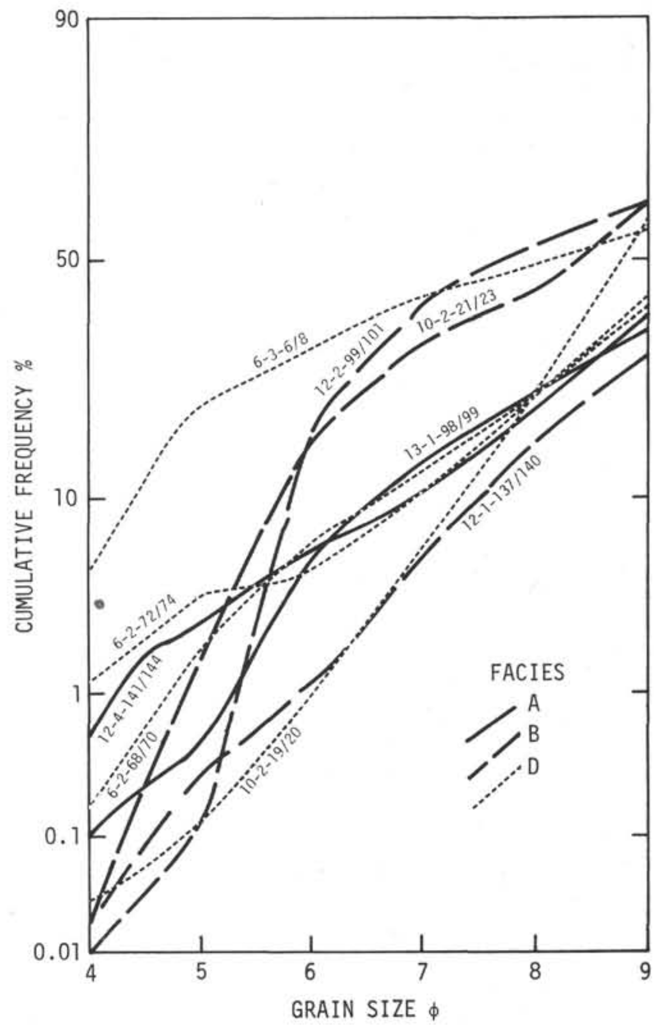

Figure 8. *Grain size analyses of clay facies A, B, and D for the lower part of Hole 269A, determined by pipette analysis.*

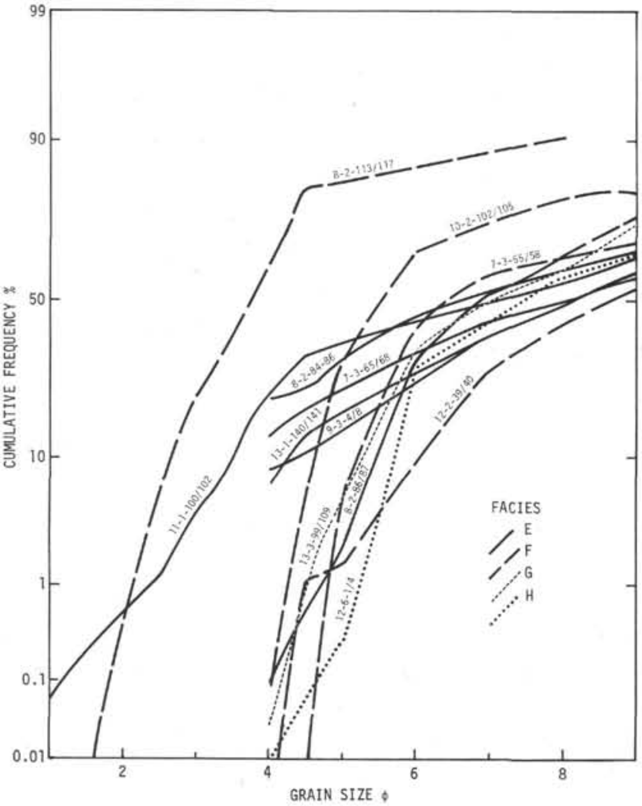

Figure 9. *Grain size analyses of silts from the lower part of Hole 269A, determined by pipette analysis and sieving.*

mottling: in this and other facies, mottling generally appears to result from bioturbation.) Sometimes a very indistinct horizontal lamination appears to be present. Organic carbon content around 0.4%.

B) **Dark brownish-gray silty claystone:** Without visible mottling. Interbedded thin silt laminae of Facies J are common, suggesting that bioturbation has not occurred. Organic carbon content around 0.4%.

C) **Dark brown mottled silty claystone:** Mottling usually moderate to intense. Organic carbon content around 0.1%.

D) **Dark greenish-gray mottled silty claystone:** Mottling usually moderate to intense. (Facies D2 is similar in color, but appears unmottled.) Organic carbon content around 0.1%.

E) **Intensely mottled coarse silt and fine sand:** This occurs in beds usually several centimeters thick. Most beds have a sharp top and are overlain by a variety of lithologies.

The beds appear to be bioturbated equivalents of facies F. They show a similar grain-size distribution of their sand component. At least one bed of facies E passes down into an unbioturbated bed of facies F. A bed in Core 13, Section 1 is distinctly graded.

F) **Silt and very fine sand beds:** Commonly cemented with calcium carbonate. Several different types have been recognized, but recognition may in part be dependent on preservation. (F1) Well-sorted fine sand and coarse silt beds, without visible structure. (F2) Beds of very fine sand and coarse silt, with cross-lamination and/or convolute lamination. The Bouma (1962) *bcd* sequence has been recognized in several beds (Figure 10). (F3) Beds of very fine sand and coarse silt, with lamination only. (F4) Beds of medium and coarse silt, with lamination, but not prominently graded. (F5) Medium and coarse silt beds, around 1 cm thick, without visible structure. (F6) Beds of medium and coarse silt, with lamination and prominent grading. Almost all of these beds have sharp bases, but a few appear to grade up from facies G and H.

G) **Laminated silts:** Comprising medium and fine silt laminae alternating with laminae of clayey siltstone. Individual laminae are 0.5-2 mm thick, with beds of this facies usually several centimeters thick. Prominent horizontal lamination is the commonest primary depositional structure, occasionally with slight scour and fill. Cross-lamination is very rare.

Synsedimentary deformational structures are ubiquitous (Figure 11). The commonest is the development of small load casts and ball and pillow structures, on the scale of about 1 mm, in individual silt laminae. Less commonly, load deformation affects composite units up to 1 cm thick. Synsedimentary faulting and extension necking or boudinage have been observed.

TABLE 1
Summary of Facies in Lower Part of Hole 269A

Facies	Brief Description	Color	Thickness (%)
A	Olive-black claystone, no mottling	5Y3/1	28.8
A2	As A, but with slight mottling	5Y3/1	2.4
B	Dark brownish-gray silty claystone, no mottling	10R4/2, 5YR4/1, 5YR3/1	29.5
C	Dark brown mottled silty claystone	5YR5/1	4.3
D	Dark greenish-gray mottled silty claystone	5G4/1, 5GY4/1, N4, N3	7.1
D2	As D, but with no mottles	(as D)	0.9
E	Intensely mottled coarse silt and fine sand		9.2
F	Beds of silt and very fine sand, no mottling		5.6
G	Finely laminated silt, often with deformational structures		3.5
H	Horizontally laminated clayey siltstone		3.1
H2	As H, but with slight mottling		0.7
I	Groups of silty laminae forming graded laminated beds		1.3[a]
J	Single or randomly grouped silt laminae		3.5[a]

[a]Thickness of sediment with abundant laminae, not total thickness of laminae.

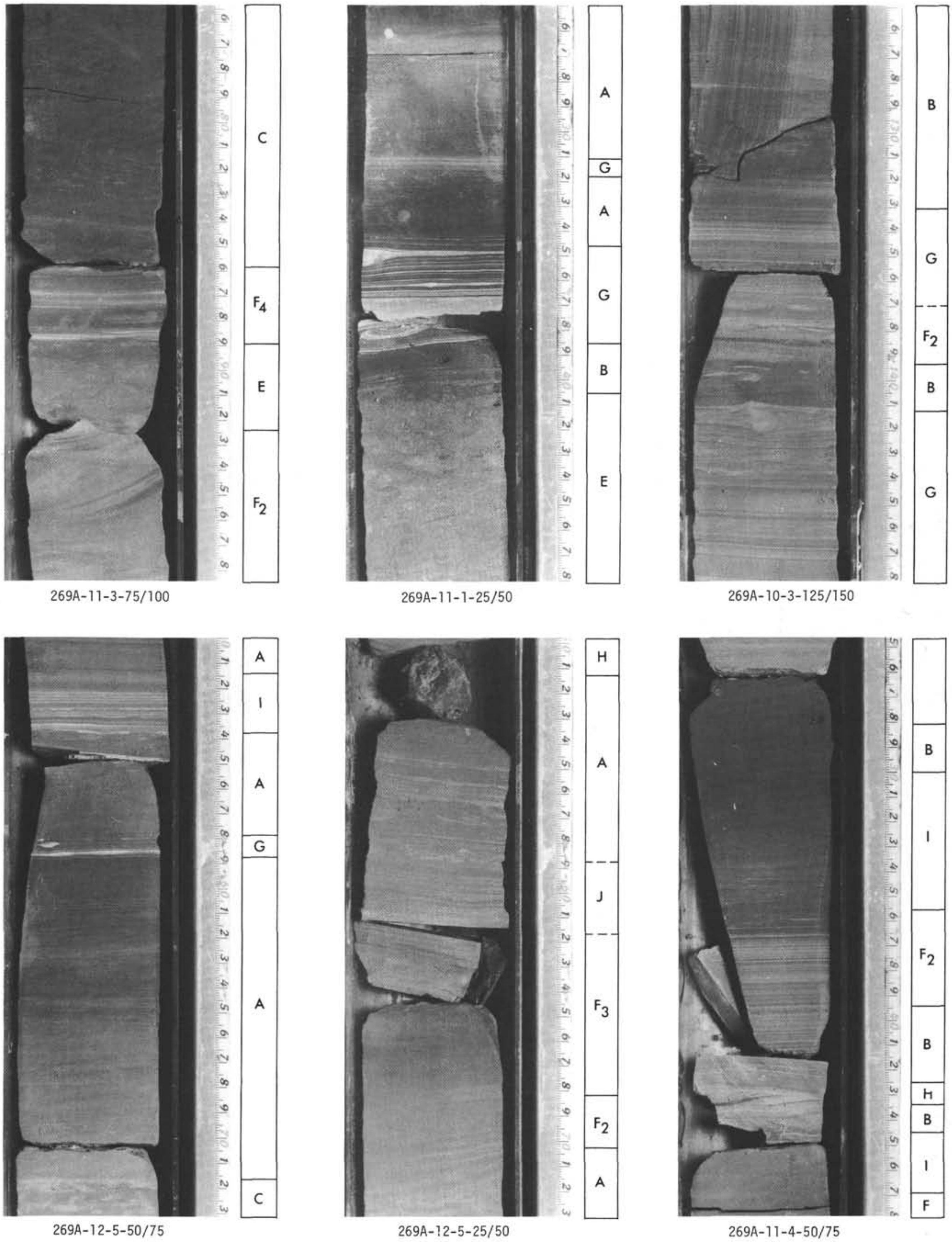

Figure 10. *Representative sequences of silty lithologies from the lower part of Hole 269A.*

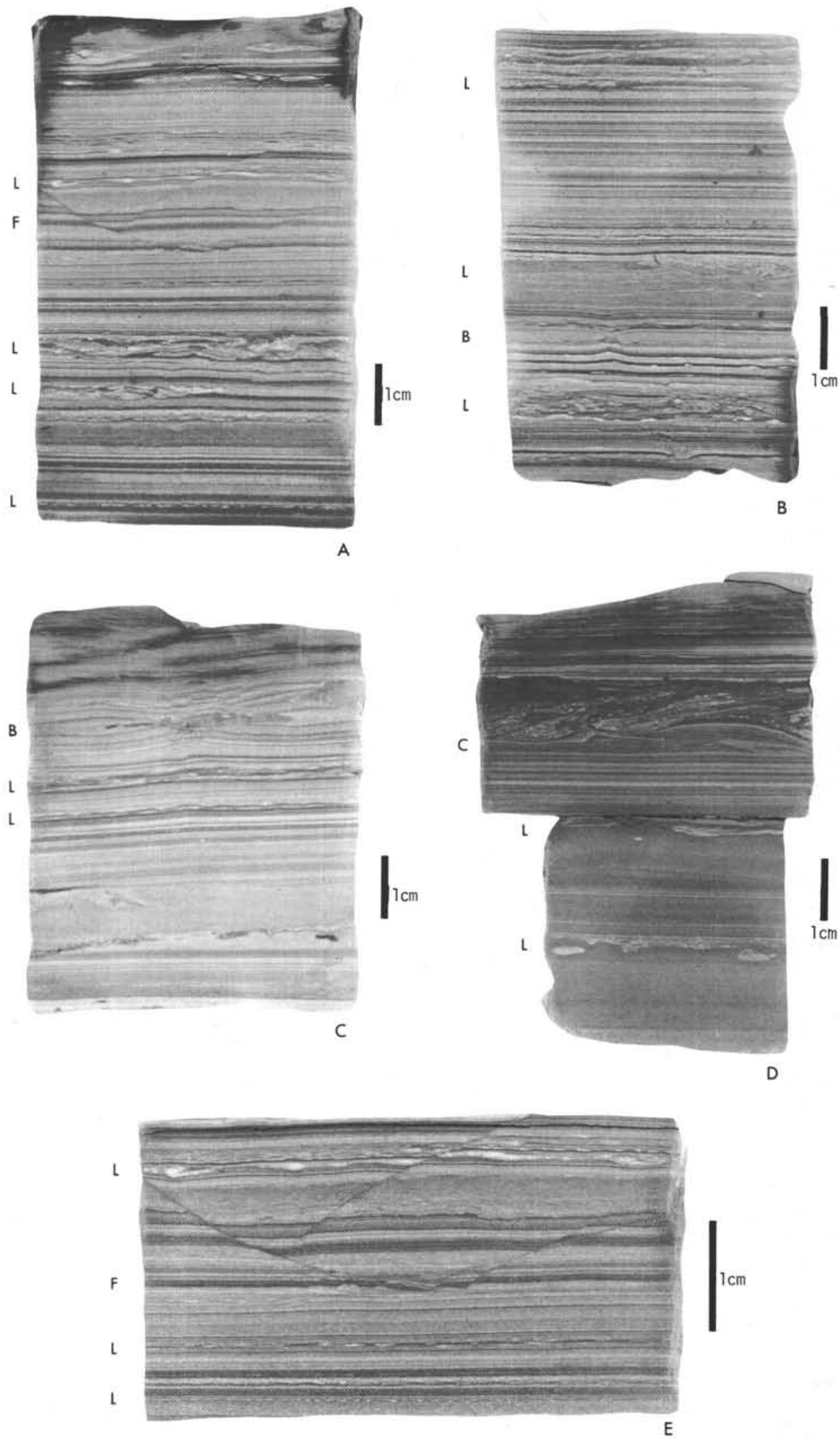

Figure 11. *Laminated deformed lithified silts of facies G, lower part of Hole 269A. Scale bar = 1 cm; B = boudinage; C = convolute lamination; G = fault; L = load deformation. (a) 269A-13-2, 120-130 cm. Shows lamination; load deformation involving both several laminae, and individual silt laminae; synsedimentary normal faulting. (b) 269A-13-3, 101-109 cm. Shows lamination; boudinage; and load deformation as in* (a). *(c) 269A-7-4, 47-69 cm. Shows massive graded silt bed of facies F; load deformation; boudinage and associated faulting. (d) 269A-7-3, 50-58 cm. Shows load casting and convolute lamination. Lower part of slab is mostly of facies H. (e) enlargement of part of* (a), *showing faulting and load casting on several scales.*

In places, the primary depositional structure appears a rather irregular lenticular discontinuous lamination. This appears a common feature of silts: it is also found in facies F and has been previously figured by Piper (1972a, fig. 4A, 4C, lower parts).

A few beds grade finer upwards, but in most the range of grain size is too small to visibly recognize grading.

H) **Clayey siltstone:** Has an indistinct horizontal lamination. Generally found in beds 1-10 cm thick, which are sometimes size graded. Facies H2 has slight mottling, but generally bioturbation mottling is absent. There appears to be a complete gradation between this facies and facies G. Load structures are not seen, and the lamination has a much less-pronounced alternation of grain size compared with facies G.

I) **Groups of silt laminae:** 0.2-2 mm thick, alternating with silty claystone, such that the abundance, thickness, and grain size of silt laminae decrease upwards. This lithology is the graded laminated bed of Piper (1972b).

This facies is similar to facies G except that load structures are rare, grading is developed, and interlaminated silty claystone tends to be commoner.

J) **Single or randomly grouped silt laminae:** Less than 1 mm thick, in silty claystone or claystone. Usually no primary structures are visible, but load structures are occasionally found.

Petrology

X-ray diffraction analysis of six clay and mud samples (three from facies A, one from B, two from D) shows no systematic differences in petrology between the clay facies, although more data would be desirable.

Silts comprise mostly quartz, with subordinate amounts of feldspar, and 0.2%-2% heavy minerals, notably hornblende, garnet, chlorite, biotite, zircon, tourmaline, and opaque minerals.

Bioturbation

Burrows are visible in facies A2, C, D, E, and H2. Few can be assigned to any distinctive trace fossil taxon. *Chondrites* occurs occasionally in facies A2 and H2 (Figure 12a, c, d). *Zoophycos* is common in facies D, and exceptionally in other facies (Figure 12c).

Burrows, often subvertical, with diameters of several millimeters, are common in facies E and associated beds of facies C and D (Figure 12b, d). They are filled with sandy muds, with sand contents of up to 20%. The grain sizes are consistent with concentration of grains from facies E. Sometimes, there remains only a thin bioturbated remanent of facies E, with none of the original bedding (Figure 13).

Facies Relationships

Preservation of structures was sufficiently good in Cores 8 through 13 of Hole 269A that the great majority of lithologic contacts were preserved unbroken. Three hundred sixty unbroken contacts (with an additional 40 broken contacts) between different lithologies were logged from well-preserved sections and used to construct a transition matrix. A simplified version of the matrix, with minor lithologies omitted (to give 332 contacts), is shown in Table 2. The data quality does not allow sophisticated mathematical analysis. A qualitative interpretation of the transition matrix is possible based on Selley's (1970) method of identifying those transitions between facies which occur much more frequently or much less frequently than would be expected in a random sequence.

Salient features of this transition matrix include: (1) Facies A and B are commonly associated with facies I and J. (2) Unbioturbated clays (facies A and B) are rarely overlain by bioturbated facies C, D, and E . With the exception of E overlain by A, the converse is also true. (3) The distribution of facies overlying facies E is almost random, but facies D is unexpectedly common. (4) Facies E generally overlies facies C or D.

Certain gradational sequences of facies observed directly from the cores provide further information on facies associations. Figure 10 shows selected short core logs showing relationships between sandy and silty facies.

Interpretation of Facies

The lack of microfossils makes interpretation of the abyssal plain sediments in this lower part of Hole 269 much more difficult than in most such sequences.

Most abyssal plains have thick beds of turbidite clay, characterized by high organic carbon contents and few microfossils. Facies A and B claystones are thought to be such turbidite clays. They are both found resting with a sharp base on highly bioturbated facies D and E, indicating an abrupt termination of bioturbational conditions. Coccoliths have been found (below the carbonate compensation depth) in three beds, suggesting resedimentation from shallower depths. The color difference between the two facies may reflect the degree of oxidation of the source material. The maximum thickness of these clay beds cannot be determined.

At least some of the thin sand and silt beds in facies F are also turbidites. Graded bedding is common; the *bcd* divisions of the Bouma sequence and convolute lamination are found; cross-lamination with no stoss side erosion is present. Foraminifera in one bed suggest resedimentation from shallower depths. The beds resemble those described by Piper (1973) from the Gulf of Alaska: sorting and clay contents are similar. In contrast to the upper part of the hole, the only sand bed analyzed contains about 10% clay.

There is, however, no evidence that many of the beds are not winnowed deposits of contour currents. Rare gradational bases of beds overlying facies G and H could be interpreted in this way.

The bioturbated sandy muds of facies E have a range of grain sizes similar to those of facies F, and they are interpreted as bioturbated equivalents. In a few cases, facies E grades down into facies F, and some beds of E grade finer upwards. The sharp upper contact of E with other facies suggests exposure on the sea floor for a period of time and that the unbioturbated original bed was not overlain by a thick mud. Although turbidite sands without an overlying mud are common, comparable silts have not been described. Thus a bottom (contour) current origin for at least some of the parent unbioturbated sands and silts is favored. However,

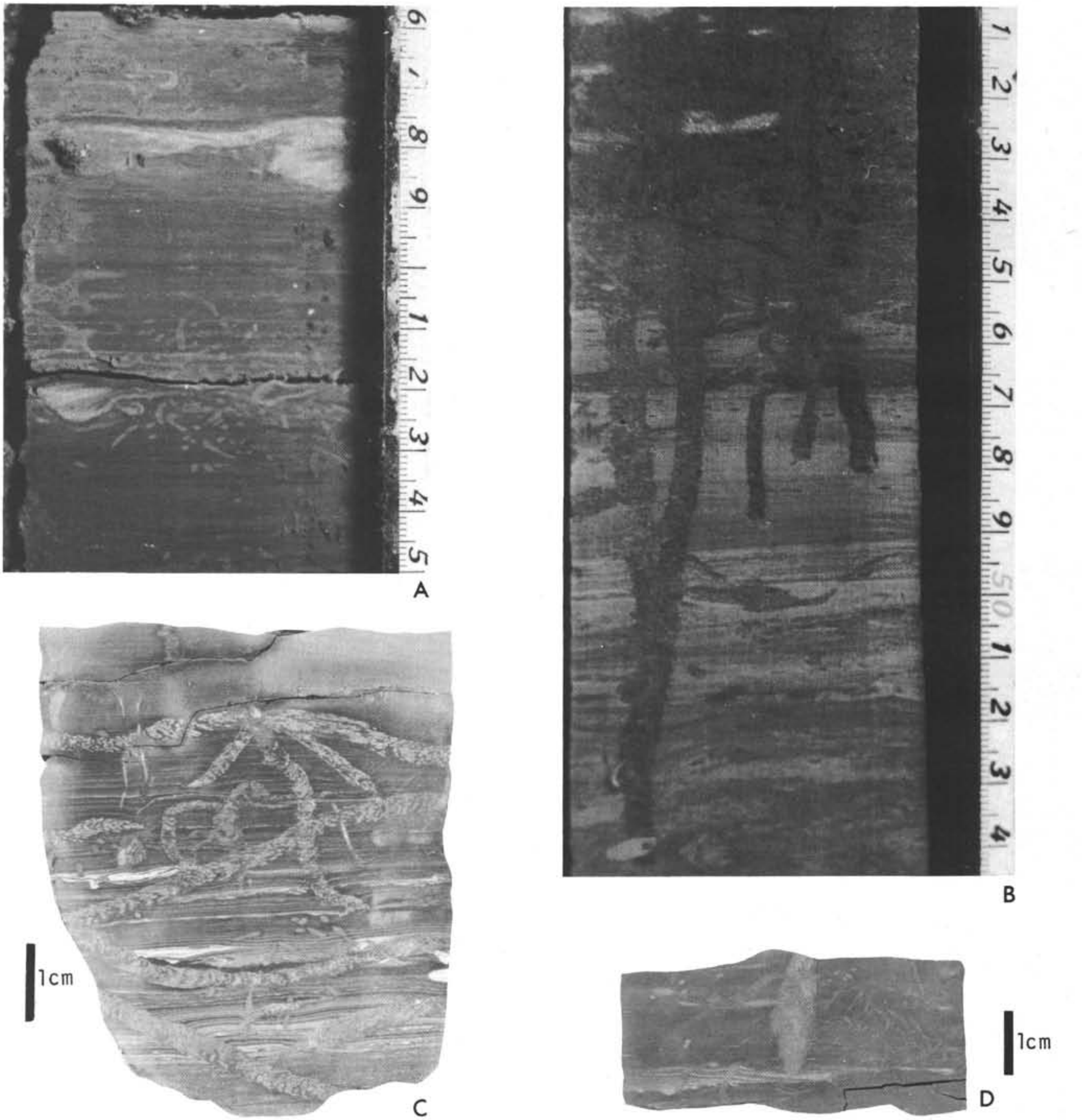

Figure 12. *Bioturbation in lower part of Hole 269A. (a) 269A-5-1, 23-38 cm. Facies A and facies F, with occasional* Chondrites. *Note ?flute mark filled with cross-laminated silt at 32 cm. (b) 269A-10-3, 40-55 cm. Long vertical burrows filled with sandy mud extending down from facies F. (c) 269A-6-3, 26-32 cm. Facies G and J, with* Zoophycos *and* Chondrites. *(d) 269A-6-3, 24-26 cm. Facies D and G, with large burrow filled with sandy mud, and* Chondrites. *Note erosional base to facies G silt bed, apparently filling small burrows, and the progressive overstep of laminae in the silt bed.*

facies D (bioturbated mud) frequently overlies facies E unexpectedly: in these cases there may have been bioturbation of an original sand and silt to mud couplet. The presence of foraminifera in one bed, and coccoliths in three, suggests resedimentation from shallower depths. Any sands or silts exposed on the sea floor for any length of time would be much more susceptible to bioturbation than muds, since larger benthos are commoner in granular sediments.

Facies G shows many examples of synsedimentary instability, which is otherwise uncommon in the sequence. This instability is most simply interpreted as the result of rapid deposition from suspension, with much pore water trapped in poorly packed silts and clays. It is in-

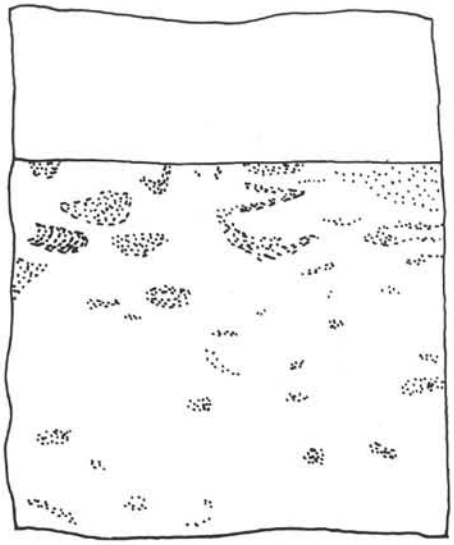

Figure 13. *Sketch from an X-radiograph of bioturbated remnant of facies E sand, overlain by unbioturbated claystone of facies B. Scale bar is 1 cm. 269A-12-2, 124-131 cm.*

conceivable that such abundant and varied deformational structures would be produced by the predominantly tractional motion of contour currents. A turbidity current could readily produce the required rapid deposition from suspension.

Facies H shows a completely gradational range of appearance with facies G, but deformational structures have not been seen. A turbidite origin is preferred.

Facies I is interpreted as turbidite solely by comparison with the examples discussed by Piper (1972b). In two cases (10-2, 96-103 cm and 11-4, 58.5 cm) individual laminae show load deformation, supporting a turbidite origin, by analogy with facies G.

Isolated or random sequences of silt laminae (Facies J) are also common in other abyssal plain sequences. They are usually sharp-based and continuous, and sometimes show load deformation. Comparing them with the lower part of Site 268, they are probably not formed by contour currents. There are insufficient data for a firm interpretation.

No interpretation is offered for the bioturbated clays and muds of facies C and D. They may be pelagic or "hemipelagic" clays, or they may be bioturbated turbidites.

Site 274

Site 274 is situated on the continental rise off Victoria Land and has an unexpectedly thin sedimentary sequence above oceanic basement. This is probably because a major graben upslope has protected it from direct sedimentation from the continental shelf for most of its history.

Only in Unit 3 are beds of sorted sand and silt found. The base of the unit is marked by a disconformity: the unit is of lower and middle Miocene age. A few of these sand and coarse silt beds (e.g., 18-3, 47-49 cm) are distinctly graded. The thicker beds, including a 3.3-meter-thick sand bed at the top of Core 18, have sharp bases, but do not appear graded. Grain-size analysis (Figure 14; Table 3) shows an almost constant median grain size through the beds, but higher percentages of fine silt and clay in the lower parts of the beds, where large Radiolaria are also concentrated. In other words, the mean grain size remains constant, but sorting improves, passing up through a bed.

Much thinner silty laminae are also found in Unit 3. Thin sections of these show the median grain size is 5-6θ. The silt laminae occur in groups which closely resemble the graded laminated beds described by Piper (1972a, 1972b). The silt laminae alternate with mud laminae in beds 0.3-2 cm thick. Each bed has a sharp base and an upward decrease in the thickness, abundance, and grain size of the silty laminae. The tops of some of the silty laminae are very sharp. In one sample (274-18-4, 48-50 cm) there is a cross-laminated silt at the base of such a bed.

ICE-RAFTING OF SEDIMENT

Introduction

Ice-rafting of sediment is manifestly an important depositional process around Antarctica. Large numbers of dispersed pebbles were found in Leg 28 holes, some in deep-water pelagic sedimentary sequences. A representative sample of a pebble population is rarely obtained in DSDP cores. Relatively small samples, however, are suitable for studying the sand fraction of the sediments. Sand has a less obvious ice-rafted origin than pebbles. Abundant sand in pelagic sediment sequences and coarse sand in "hemipelagic" sequences, in the absence of distinct current-concentrated sand beds, are interpreted as being ice-rafted in origin. Specific cores where this interpretation is critical are discussed in detail below.

Methods

The methods used are based on those described by von Huene et al. (1973). Channel samples were taken by cutting out a narrow groove of sediment with a spatula from a 50-cm length of core. Disturbed lengths of core were avoided. Sample size was around 10 g of dry sediment.

Sediments were disaggregated with hydrogen peroxide and Calgon and ultrasonic treatment where necessary. They were then wet sieved through a 2ϕ (250μ) and 4ϕ (63μ) screen to determine the amounts of "coarse" and "fine" sand. The silt and clay fraction was determined by conventional pipette analysis. Any pebbles (>4 mm) were removed by hand.

The sand fractions were dried and weighed and the proportion of detrital grains estimated. Many samples in addition contained larger diatoms, Radiolaria, ferromanganese nodules, and sometimes undispersed clay aggregates. Where very few detrital grains were present, they were individually counted while still on the sieve, using a binocular microscope. Sieves were cleaned in an

TABLE 2
Transition Matrix Between the Principal Facies in the Lower Part of Hole 269

Observed Transitions

Upper Bed

		A	B	C	D	E	F	G	H	I	J	
	A		3	2	2	1	8	11	7	3	17	54
	B	0		1	2	3	16	10	10	3	27	72
	C	1	2		2	7	1	0	0	0	1	14
	D	2	0	0		9	3	1	0	0	1	16
Lower	E	4	4	1	4		4	0	1	1	0	19
Bed	F	7	10	2	5	0		2	4	6	6	42
	G	10	12	0	3	1	0		0	0	0	26
	H	9	9	2	1	0	3	0		1	1	26
	I	2	8	2	0	0	0	0	0		0	12
	J	15	26	1	3	0	2	2	2	0		51
		50	74	11	22	21	37	26	24	14	53	332

Number of Transitions Predicted if Random

Upper Bed

		A	B	C	D	E	F	G	H	I	J
	A		12.0	1.8	3.6	3.4	6.0	4.2	3.9	2.3	8.6
	B	10.8		2.4	4.8	4.6	8.0	5.6	5.2	3.0	11.5
	C	2.1	3.1		0.9	0.9	1.6	1.1	1.0	0.6	2.2
	D	2.4	3.6	0.5		1.0	1.8	1.3	1.2	0.7	2.6
Lower	E	2.9	4.2	0.6	1.3		2.1	1.5	1.4	0.8	3.0
Bed	F	6.3	9.4	1.4	2.8	2.7		3.3	3.0	1.8	6.7
	G	3.9	5.8	0.9	1.8	1.6	2.9		1.9	1.1	4.2
	H	3.9	5.8	0.9	1.8	1.6	2.9	2.0		1.1	4.2
	I	1.8	2.7	0.4	0.8	0.8	1.3	0.9	0.7		1.9
	J	7.7	11.4	1.7	3.3	3.2	5.7	4.0	3.7	2.7	

ultrasonic bath and checked under a binocular microscope after every sample when analyzing those samples with low detrital grain contents. (In some sand-rich sequences and for some preliminary analyses, cleaning was less rigorous.) Some carbonate ooze samples were treated with acetic acid, sieved, and the sand grains counted. It was found to be very difficult to recognize small quantities of sand in a diatom-rich sediment.

Evidence of Earliest Ice Rafting

Site 274

This site has an unusually complete stratigraphic sequence. It is situated on the continental rise, but at most times was protected from downslope sedimentation from the continent by a structural trough. Most of the sediment has a high biogenous component.

In the upper 113 meters (Quaternary to upper Miocene) coarse sand and pebbles are common. Below this, to 180 meters (middle and lower Miocene), most of the sediment is highly biogenous, but contains between 1% and 0.01% sand, including a few grains of coarse sand. Except at a few restricted horizons (e.g., Core 18, Section 2), there is no evidence of tractional emplacement of the sand by currents. The thick diamictites of the Ross Sea, only 500 km to the south, are time equivalents of this sequence.

From 180 to 225 meters (middle Oligocene to upper lower Oligocene) extremely rare sand grains are found in the sediment. None have been found below this. The grains are too small to show diagnostic surface textures under the scanning electron microscope. The Ross Sea holes do not indicate glaciation at the time this sequence accumulated. Such very small amounts of sand could well have been emplaced by processes other than ice-rafting.

Site 269

Granules and pebbles are exceptionally found in the uppermost two cores (Plio-Pleistocene) of this site. Because of the abundance of trubidites at this site, sand distribution cannot be used as evidence of ice-rafting.

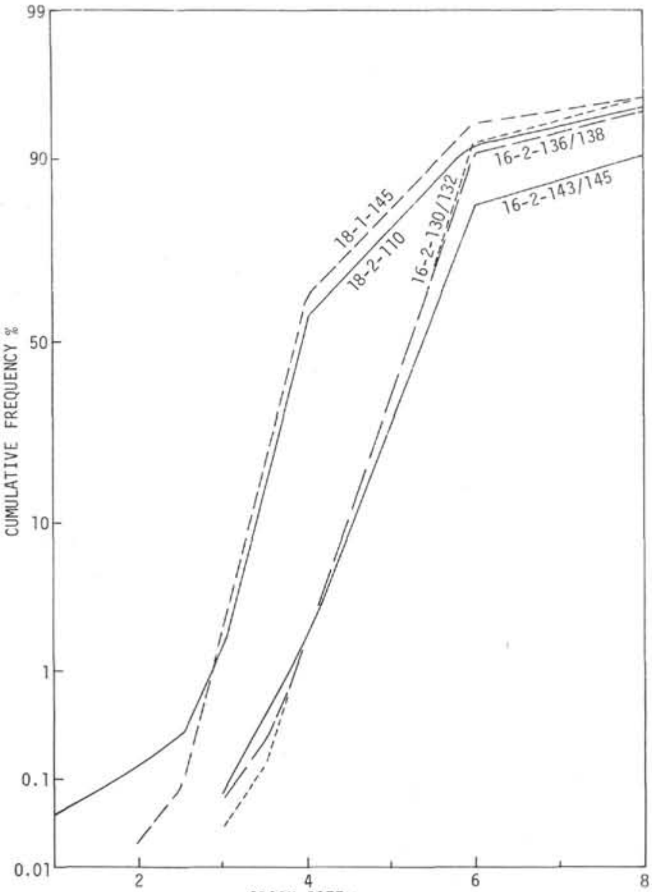

Figure 14. *Grain size analyses of turbidite silt beds from Site 274. (a) Near base, and from upper part of 2.7-meter thick sand bed in Core 18 (base at 274-18-2, 120). Compare with Table 3. (b) Samples from middle and lower part of a 40-cm-thick silt bed, grading up into 50 cm alternating silt and clay (base at 274-16-2, 146).*

TABLE 3
Grain Size Analyses From a Single Bed at Site 278

Sample (Interval in cm)	Percent Finer Than 2ϕ	4ϕ	6ϕ	8ϕ
18-1, 120-122	0.03	64.1	94.6	96.3
18-1, 145-147	0.02	61.7	93.4	95.5
18-2, 20-22	0.03	62.8	93.1	95.9
18-2, 50-52	0.01	65.0	93.8	96.2
18-2, 80-82	0.27	67.1	91.7	95.3
18-2, 110-112	0.14	64.0	91.3	96.8

Site 268

This is a normal continental rise site, so that bottom transport of coarse sand is not unlikely. Induration and chertification hinders analysis. It is difficult to obtain uncontaminated soft sediment from short cores which consist mostly of short blocks of indurated sediment.

Ice-rafting is well established down to Core 10 (middle lower Miocene), with high percentages of dispersed sand. Below this, a little sand is still found in abundances comparable with those at Wite 274 between 180 and 225 meters: its origin is uncertain. In Core 14 there is a single granite pebble: this could be downhole contamination, as in Cores 22-34 at Site 274. A chert in Core 19 (pre-middle Oligocene) has an irregular layer of granules and coarse sand grains. These are not sufficiently dispersed to be considered as ice-rafted, nor sufficiently bedded to be due to bottom or turbidity currents. Their origin is uncertain.

Site 267

Ice-rafted sand and pebbles are found in the Pliocene and Quaternary sequence at Site 267. The Miocene sediments are generally rich in siliceous organisms and no sand was detected. Acid residues of upper Oligocene carbonate ooze from Core 4 contained a few sand grains, which may indicate ice-rafting.

Site 266

This is a fully pelagic site, well away from the abyssal plain. Small amounts of detrital sand are found in many samples down to 157 meters (upper Miocene), although some samples are barren. Below this, acid residues of all but one of the samples analyzed contained no sand. The three quartz sand grains in Core 20, Section 4 may be due to contamination.

Summary

In the Ross Sea sector, the data from Site 274 substantiate the evidence from the Ross Sea sites that significant glaciation was initiated in the late Oligocene. The significance of trace amounts of sand in the early Oligocene is unclear.

In the Wilkes Land sector, there is unequivocal evidence of early Miocene, and possible evidence of late Oligocene ice-rafting. Earlier minor ice-rafting cannot be ruled out.

Grain-Size Distribution of Ice-Rafted Sediment

Grain-size distribution of ice-rafted sand and larger clasts is very variable, even at any one site. This variation is best documented at Sites 274 and 270 (Barrett, Chapter 22). In the grain size analyses in Table 4, the variation can be recognized from differences in the ratio of coarse to fine sand. (However, this statistic is probably unreliable in siliceous oozes with low detrital grain contents. It is much easier to see a coarse sand grain in an otherwise empty 2ϕ sieve than a fine sand grain in a 4ϕ sieve full of diatoms.)

Barrett (Textural Characteristics of Cenozoic Preglacial and Glacial Sediments, this volume) has shown that grain-size variations at Site 270 do not appear to be the result of variations in the petrology of source material; and that diamictites both with high and with low proportions of coarse sand and pebbles are equally poorly sorted. The pebble-rich diamictites cannot be the result of sea-floor winnowing of granule-poor diamictites.

At Site 274, Cores 10-12 are unusually rich in coarse sand. Above Core 10, there is a spectrum of coarse to fine sand ratios, but it is generally lower than in Cores

TABLE 4
Size Analyses of Channel Samples From Sites 266, 267, 268, 269, 272, and 274

Sample (Interval in cm)	Depth (m)	Clay (%)		Silt (%)	Sand (%)	Detrital Sand (%) >2ϕ	Detrital Sand (%) 2-4ϕ
Site 266							
1-3, 100-150	4.0-4.5	56.35		41.34	2.31	tr	0.04
2-2, 90-92	31.9-31.92	54.12		36.55	9.33	0.0	0.0
3-1, 100-150	45.0-45.5	48.75		49.48	1.77	4 grains	0.0
4-4, 50-100	71.0-71.5	57.22		42.08	0.70	3 grains	1 grain
5-6, 50-100	90.0-90.5	79.84		19.01	1.15	6 grains	0.02
6-5, 50-100	107.5-108.0	75.09		23.11	1.79	0.0	0.02
7-5, 50-100	128.0-128.5	18.49		80.00	1.51	0.02	0.0
8-6, 50-100	137.5-138.0	32.07		66.47	1.46	5 grains	0.0
9-4, 70-150	147.2-148.0	24.18		74.71	1.11	0.03	0.0
10-6, 50-100	156.5-157.0	78.76		20.76	0.48	tr?	0.02
11-7, 50-100	166.0-166.5	87.21		12.53	0.25	0.0	0.0
12-3, 0-40	184.5-184.9	14.84		84.91	0.25	0.0	0.0
13-3, 50-100	199.5-200.0					0.0	0.0
14-4, 0-50	219.5-200.0					0.0	0.0
15-2, 0-50	235.5-236.0					0.0	0.0
16-2, 100-150	246.0-246.5					0.0	0.0
17-5, 0-50	260.5-261.0	28.53		71.14	0.33	0.0	0.0
20-4, 52-54	318.5					1 grain	2 grains
22-2, 50-52	363.0					0.0	0.0
Site 267							
1-3, 90-150	3.5-4.0	59.88		29.85	10.27	1.23	0.20
3-3, 50-100	93.5-94.0					0.0	0.0
4-1, 50-100	128.5-129.0					2 grains	0.0
4-3, 50-100	131.5-132.0					0.0	7 grains
1A-1, 50-100	4.5-5.0	68.95		30.08	1.37	0.05	0.04
1A-1, 100-150	5.0-5.5	63.95		34.28	1.77	0.13	0.72
1A-2, 0-50	5.5-6.0		98.75		1.25	0.19	0.38
1A-2, 50-100	6.0-6.5		97.20		2.80	1.32	0.20
1A-2, 100-150	6.5-7.0		98.86		1.14	0.58	0.16
1A-3, 0-50	7.0-7.5	53.56		44.49	1.95	0.21	0.30
1A-3, 50-100	7.5-8.0		96.81		3.19	0.19	0.18
1A-3, 100-150	8.0-8.5	50.64		42.73	6.64	0.21	1.12
1A-4, 0-50	8.5-9.0		97.97		2.03	0.67	0.21
1A-4, 50-100	9.0-9.5		98.66		1.34	0.22	0.10
1A-4, 100-150	9.5-10.0		98.85		1.15	0.40	0.12
1A-5, 0-50	10.0-10.5	50.73		47.77	1.50	0.08	0.12
1A-5, 50-100	10.5-11.0	47.91		50.22	1.86	0.14	0.02
1A-5, 100-150	11.0-11.5	62.09		34.94	2.96	1.60	0.02
1A-6, 10-50	11.6-12.0	75.27		23.00	1.73	0.18	0.21
1A-6, 50-100	12.0-12.5	79.22		18.49	2.29	0.05	0.04
1A-6, 100-150	12.5-13.0	68.24		21.16	10.60	2.58	0.08
3A-2, 100-150	70.0-70.5		98.98		1.02	0.0	0.0
1B-1, 45-90	113.5-114.0	31.56		68.37	0.07	5 grains	1 grain
2B-1, 110-150	142.5-143.0		99.48		0.52	0.10	0.07
3B-2, 113-150	152.0-152.5		99.96		0.04	0.0	0.0
4B-3, 59-150	171.0-171.5		97.69		2.31	0.0	0.0
5B-6, 50-100	189.5-190.0		99.55		0.45	0.0	0.0
1-2, 90-100	2.4-2.5	10.09		87.60	2.31	0.79	0.35
1-3, 0-46	3.0-3.5		98.07		1.93	0.80	0.95
2-1, 43-100	28.43-29.0	52.22		16.70	21.08	24.41	3.00
2-4, 72-90	33.2-33.9	67.05		31.26	1.69	0.75	0.37
2-5, 50-101	34.5-35.1	76.70		23.00	0.30	0.14	0.14
2-6, 60-100	36.1-36.5	62.96		19.76	3.33	1.59	1.21
3-1, 60-100	57.1-57.5	62.96		34.97	2.07	0.78	1.28
3-2, 65-100	58.7-59.0	57.09		32.65	10.26	5.88	4.28
4-2, 50-100	87.0-87.5	67.00		26.31	6.69	4.77	1.14
5-1, 45-95	113.9-114.4	64.54		25.16	10.30	3.53	0.63
5-2, 50-100	115.5-116.0	61.10		16.51	22.39	8.37	12.16
7-2, 50-100	146.0-146.5	69.00		25.80	5.20	1.33	1.68
8-2, 55-96	172.5-172.9	79.58		19.80	0.62	0.18	0.08
8-3, 60-110	174.1-174.6	80.47		18.33	1.20	0.82	0.04
9-1, 60-100	199.6-200.0	73.04		20.37	6.60	2.46	2.73
10-2, 50-100	229.5-230.0		99.89		0.11	0.05	0.03
12-1, 100-150	285.5-286.0	51.01		48.87	0.11	0.02	0.02
17-3, 95-150	388.5-389.0					0.0	0.0
18-2, 70-100	410.2-410.5	62.34		37.50	0.15	0.0	0.01
18-3, 85-115	411.85-412.15	70.37		29.50	0.12	0.0	tr

TABLE 4 – *Continued*

Sample (Interval in cm)	Depth (m)	Clay (%)		Silt (%)	Sand (%)	Detrital Sand (%) >2ϕ	Detrital Sand (%) 2-4ϕ
Site 269							
1-3, 100-150	4.0-4.5	52.12		44.07	3.80	0.21	0.08(?)
Site 272							
1-1, 80-110	4.8-5.1	62.57		29.13	8.29	5.33	2.96
1-2, 50-100	6.0-6.5	23.78		28.53	57.69	27.10	13.81
1-3, 50-100	7.5-8.0	37.47		28.49	34.05	17.63	11.59
1-4, 50-100	9.0-9.5	40.25		27.34	32.41	14.27	14.57
1-5, 50-100	10.5-11.0	41.23		28.00	30.76	15.14	15.32
2-2, 50-100	17.0-17.5	31.82		25.18	42.99	21.84	13.75
2-3, 50-100	18.5-19.0	34.44		23.70	41.85	22.52	15.39
2-4, 50-100	20.0-20.5	32.77		25.56	41.67	17.23	17.02
2-5, 50-100	21.5-22.0	31.64		24.95	43.41	26.07	16.52
3-1, 50-100	26.5-27.0	39.74		32.32	27.95	8.52	19.42
Site 274							
1-2, 50-100	2.0-2.5	56.75		39.68	3.57	0.34	0.24
1-3, 50-100	3.5-4.0		99.07		1.01	0.19	0.55
1-4, 50-100	5.0-5.5	63.53		34.10	2.37	0.60	0.75
1-6, 50-100	8.0-8.5	54.26		40.23	5.52	2.66	1.72
2-2, 50-100	11.5-12.0	66.01		32.19	1.80	0.49	0.44
2-3, 50-100	13.0-13.5	48.32		50.27	1.41	0.27	0.14
2-4, 50-100	14.5-15.0	61.16		35.49	3.35	0.91	0.24
2-5, 50-100	16.0-16.5	57.75		35.12	7.14	0.22	0.09
2-6, 50-100	17.5-18.0	60.48		38.71	0.81	0.10	0.14
3-2, 50-100	21.0-21.5	58.79		40.05	1.16	0.61	0.14
3-3, 50-100	22.5-23.0	62.83		36.71	0.47	0.05	0.06
3-4, 50-100	24.0-24.5	65.78		32.08	2.14	1.27	0.57
3-5, 50-100	25.5-26.0	63.44		34.57	1.99	0.73	1.08
3-6, 50-100	27.0-27.5	60.61		34.29	5.09	2.49	2.60
4-1, 50-100	35.5-36.0	70.24		27.96	1.80	0.73	0.86
4-2, 50-100	37.0-37.5	73.49		25.42	1.09	0.41	0.67
5-2, 50-100	44.5-45.0	61.53		32.99	5.47	2.72	1.93
6-1, 50-100	48.0-48.5	70.13		28.34	1.53	0.63	0.81
6-2, 50-100	49.5-50.0	60.84		38.18	0.98	0.20	0.39
6-3, 50-100	51.0-51.5	61.85		36.72	1.43	0.22	0.20
6-4, 50-100	52.5-53.0	59.69		39.42	0.90	0.20	0.13
6-5, 50-100	54.0-54.5	64.38		31.90	3.72	1.72	1.99
6-6, 50-100	55.5-56.0	67.78		30.76	1.45	0.87	0.57
7-1, 50-100	63.5-64.0	73.37		25.87	1.76	0.70	0.19
7-2, 50-100	65.0-65.5	64.77		28.61	6.62	2.65	2.63
9-1, 50-100	76.5-77.0	57.90		30.12	11.99	4.61	4.40
9-2, 50-100	78.0-78.5	71.81		24.63	3.56	1.73	1.63
9-3, 50-100	79.5-80.0	60.08		29.03	10.89	4.62	5.61
9-4, 0-50	80.5-81.0		95.70		4.30	2.10	2.0
9-4, 50-100	81.0-81.5	70.91		25.00	4.09	1.45	2.11
9-5, 50-100	82.5-83.0	72.64		22.94	4.42	2.10	2.27
9-6, 0-50	83.5-84.0		93.95		6.05	2.68	2.65
9-6, 50-100	84.0-84.5	65.47		23.25	11.28	5.85	5.16
10-2, 50-100	87.5-88.0	66.01		24.58	9.41	4.30	1.00
10-2, 100-150	88.0-88.5		90.03		9.97	4.73	1.04
10-3, 50-100	89.0-89.5	68.83		22.47	8.71	3.67	1.99
10-4, 50-100	90.5-91.0	71.80		20.82	7.38	3.53	0.97
10-5, 0-50	91.5-92.0		91.10		8.90	3.79	3.96
10-5, 50-100	92.0-92.5	71.13		20.05	8.82	2.64	1.81
10-6, 50-100	93.5-94.0	69.58		23.00	7.43	1.99	1.78
11-2, 50-100	100.0-100.5		81.80		18.20	7.27	3.24
11-3, 50-100	101.5-102.0	69.68		22.32	8.00	2.28	0.42
11-4, 0-50	102.5-103.0		93.75		6.25	2.47	0.38
11-4, 50-100	103.0-103.5	64.75		27.35	7.91	2.53	2.31
12-2, 50-100	106.5-107.0	54.75		30.60	14.65	5.30	3.93
12-3, 50-100	108.0-108.5	57.44		28.33	14.22	6.73	4.42
12-4, 50-100	109.5-110.0	55.74		31.10	13.17	5.49	4.59
12-5, 50-100	111.0-111.5	52.60		31.58	15.82	6.59	5.53
12-6, 50-100	112.5-113.0	28.86		53.58	17.56	6.05	6.83
13-1, 40-100	114.4-115.0		98.44		1.56	1 grain	0.04
13-2, 50-100	116.0-116.5	62.68		33.41	3.90	2 grains	0.04
13-3, 50-100	117.5-118.0	66.36		32.49	1.10	3 grains	0.0
13-4, 50-100	119.0-119.5	64.58		33.34	2.09	3 grains	1.63
13-5, 50-100	120.5-121.0	69.56		30.39	0.05	3 grains	0.001
13-6, 50-100	122.0-122.5		99.92		0.08	tr	0.02

TABLE 4 – *Continued*

Sample (Interval in cm)	Depth (m)	Clay (%)		Silt (%)	Sand (%)	Detrital Sand (%) >2ϕ	Detrital Sand (%) 2-4ϕ
Site 274 – *Continued*							
14-1, 50-100	124.0-124.5		98.99		1.01	1 grain	0.01
14-2, 50-100	125.5-126.0	66.26		33.69	0.04	0.0	0.01
14-3, 50-100	127.0-127.5	71.85		28.14	0.02	0.0	0.01
14-4, 50-100	128.5-129.0		99.07		0.03	0.0	0.003
14-5, 50-100	130.0-130.5	72.99		26.96	0.05	0.0	0.01
14-6, 50-100	131.5-132.0	70.74		28.98	0.28	1 grain	0.03
15-2, 50-100	135.0-135.5	61.20		38.69	0.11	tr	0.04
15-3, 100-150	137.0-137.5		99.99		0.01	0.0	tr
15-4, 50-100	138.0-138.5	52.14		47.73	0.13	0.005	0.01
15-5, 50-100	139.5-140.0					0.0	?
15-6, 50-100	141.0-141.5	73.91		26.03	0.06	0.0	0.02
16-3, 50-100	151.0-151.5	55.10		42.51	2.40	1 grain	0.71
17-2, 50-100	158.5-159.0		99.98		0.02	0.0	0.02
17-3, 50-100	160.0-160.5		99.52		0.48	0.0	0.45
18-5, 50-100	169.5-170.0		99.78		0.22	1 grain	0.15
18-5, 100-150	170.0-170.5		99.84		0.16	2 grains	0.13
19-2, 50-100	173.0-173.5		99.91		0.09	1 grain	0.08
19-6, 50-100	179.0-179.5		99.93		0.07	0.0	0.06
20-5, 50-100	187.0-187.5	74.27		25.52	0.21	0.0	tr
21-6, 50-100	198.0-198.5		99.95		0.05	0.0	tr
21-6, 100-150	198.5-199.0	12.82		86.95	0.23	0.0	4 grains
22-5, 0-50	207.0-207.5	9.25		90.25	0.51	0.0	3 grains
22-5, 100-150	208.0-208.5		99.79		0.21	0.0	0.0
23-5, 50-100	215.5-216.0		99.37		0.63	0.0	tr
23-6, 50-100	217.0-217.5	19.73		89.37	0.90	0.0	0.0
24-5, 0-50	224.5-225.0	8.25		91.52	0.23	0.0	3 grains
24-5, 50-100	225.0-225.5	7.29		92.52	0.19	0.0	tr
25-6, 50-100	236.0-236.5	15.92		82.89	1.19	0.0	0.0
26-6, 50-100	245.5-246.0	8.33		91.11	0.56	2 grains volcanic glass	1 grain volcanic glass
26-6, 100-150	246.0-246.5		99.89		0.11	0.0	0.0
27-4, 50-100	255.5-256.0	6.20		93.41	0.39	0.0	0.0
28-6, 50-100	264.5-265.0	8.30		91.35	0.17	0.0	0.0
29-3, 50-100	274.0-274.5	8.88		90.70	0.43	0.0	0.0
30-6, 0-50	283.0-283.5	11.44		88.06	0.50	0.0	tr
30-6, 50-100	283.5-284.0	6.81		92.77	0.42	3 grains[a]	0.0
30-6, 100-150	284.0-284.5		99.34		0.66	0.0	0.0
31-6, 50-100	293.0-293.5	8.11		91.67	0.22	0.0	0.0
32-6, 50-100	302.5-303.0	14.21		85.36	0.43	2 grains[a]	0.0
32-6, 100-150	303.0-303.5	12.86		86.80	0.33	0.0	0.0
33-6, 50-100	312.0-312.5	5.71		93.73	0.56	0.0	0.0
34-6, 50-100	321.5-322.0	6.37		93.13	0.50	0.0	0.0

Note: Determined by conventional wet-sieve and pipette techniques. Percent sand includes gravel-size material and sand-sized, detrital, biogenic, and authigenic components; the proportion of detrital material in the sand fraction (finer than 4 mm) has been estimated using a binocular microscope. tr = trace.

[a]Early analysis in which contamination was less carefully avoided – believed due to contamination.

10-12. As at Site 270, sediments with both a high and a low coarse to fine sand ratio are equally poorly sorted. Grain-size analyses (Figure 15) show no evidence of winnowing. Neither is there evidence to suggest petrologic control of grain-size distribution.

There are several possible explanations for this type of variation. One is a control of available grain size by petrology and weathering of source material that is so subtle that it cannot be recognized from an examination of the petrology of the sedimentary sequence. Variations between sites may largely result from differences in source material.

Winnowing at or near the depositional site seems improbable from the grain-size data. However, the sediment could result from mixing of two different types of poorly sorted glacial debris in different proportions, one with a high content of sand and pebbles, the other rich in silt and clay. So long as both parent sediments were poorly sorted, it would be very difficult to distinguish distinct modes resulting from mixing. Two such parent sediments might be englacial material, little modified by the action of melt water, and till, which has had some fine material winnowed out by running water during ablation (probably while being transported in a supraglacial position).

The proportion of clay-rich till to sand-rich till will tend to vary from berg to berg. Mixing on the sea floor will result from successive dumping of material by

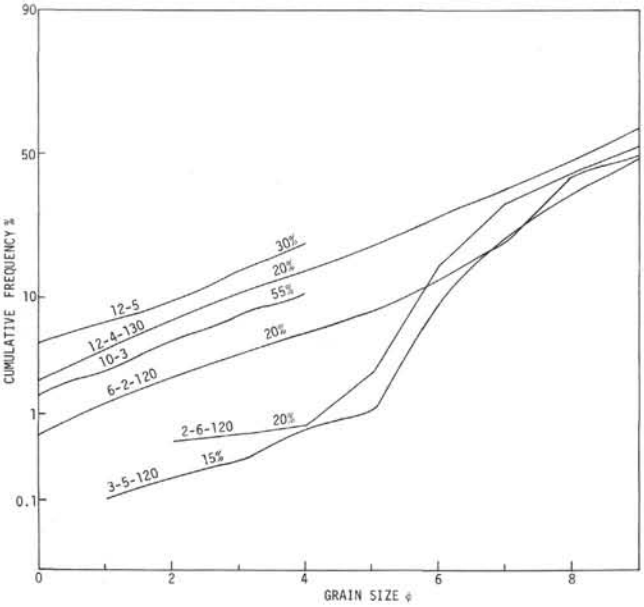

Figure 15. *Grain size analyses of sediments in upper part of Site 274. Sediment mostly emplaced by ice rafting, but in part biogenic. Percentage of biogenic components (estimated from smear slides) is indicated.*

icebergs carrying varying amounts of these two parent sediments.

Rates of Ice-Rafted Sedimentation

Because of discontinuous coring and poor paleontologic control, it is not possible to make any more than general estimates of the rate of ice-rafted sedimentation. It is difficult to distinguish ice-rafted silt and clay, and the very small amounts of coarse sand and pebbles in many cores may not be representative samples. In Figure 16, we have attempted to show variations through time in the rate of sedimentation of ice-rafted 2θ-4θ sand. Note that this grain size does not form a constant proportion of the total ice-rafted sediment. Furthermore, it could be argued that the biostratigraphic control is inadequate for this type of compilation. We have found that the several versions of this figure that were produced, as biostratigraphic correlation was modified and refined, have varied substantially in detail, but have still showed the same general trends. An equally serious problem is the lack of recovered core in some critical intervals. So the figure must be regarded as highly speculative.

In both the Wilkes Land and Ross Sea sectors, the highest rate is found in Gauss times. Rather lower rates are found in younger sediments. Our dating is not sufficiently refined to detect the type of variations seen by Fillon (1972). Gilbert (early Pliocene) rates at Sites 266 and 267 appear low. Dating is poor at Site 268; the abundance of ice-rafted sand decreases downwards in the Gauss-Gilbert interval but there is no information on overall rates of sedimentation. At Site 274, the Gauss rate may have been underestimated, or Gauss sediments may not have been recovered. Note that the core catcher of Core 8 (the only material recovered), of probable Gauss age, contained unusually pebbly sediment. The sudden appearance in Site 274, Core 12 of abundant ice-rafted sediment above middle Miocene strata with little ice-rafting is exaggerated by the very low overall rate of sedimentation in the late Miocene. The early Miocene rate of ice-rafted sedimentation is much higher than that in the middle Miocene. The middle and late Miocene at

TABLE 5
Core Sections Containing Micronodules at Sites 266, 267, 268, 272, and 274

Sample (Interval in cm)	Abundance	Type	Age
Site 266			
3-1	T		Pleistocene
4-4	T		Plio-Pleistocene
5-6	F		
8, CC	*	Dark	Pliocene
9-3	*		
10-6	F		Upper Miocene
11-6	F		Middle Miocene
(No routine examination below Core 12)			
Site 267A			
1-1, 50-100	T		
1-1, 100-150	T		
1-2, 0-50	F		
1-2, 50-100	F		
1-2, 100-150	F		
1-3, 0-50	F		
1-3, 50-100	M		
1-3, 100-150	F	Dark	Plio-Pleistocene
1-4, 0-50	F		
1-4, 50-100	M		
1-4, 100-150	M		
1-5, 0-50	M		
1-5, 50-100	M		
1-5, 100-150	M		
1-6, 0-10	Manganese-oxide-coated pebble bed		
1-6, 10-50	F		
1-6, 50-100	T		Pliocene
1-6, 100-150	M		
Site 268			
1-2	F		
1-3	M		
2-6	F	Light	Pleistocene
3-1	F		
3-2	T		
(No routine examination below Core 12)			
Site 272			
1-5	F		
2-2	F	Light	Plio-Pleistocene
2-5	F		
(No routine examination below Core 3 Section 1)			
Site 274			
10-2 through			Pliocene to
12-3	F	Dark	middle Miocene
Macronodules from 10-5 through 12-6			

Note: T = trace; F = few (1-5% of sand fraction); M = many (>5% of sand fraction); * in smear slides, but not in adjacent sand fractions. Based on examination of sand fractions of all grain-size analyses reported in this chapter.

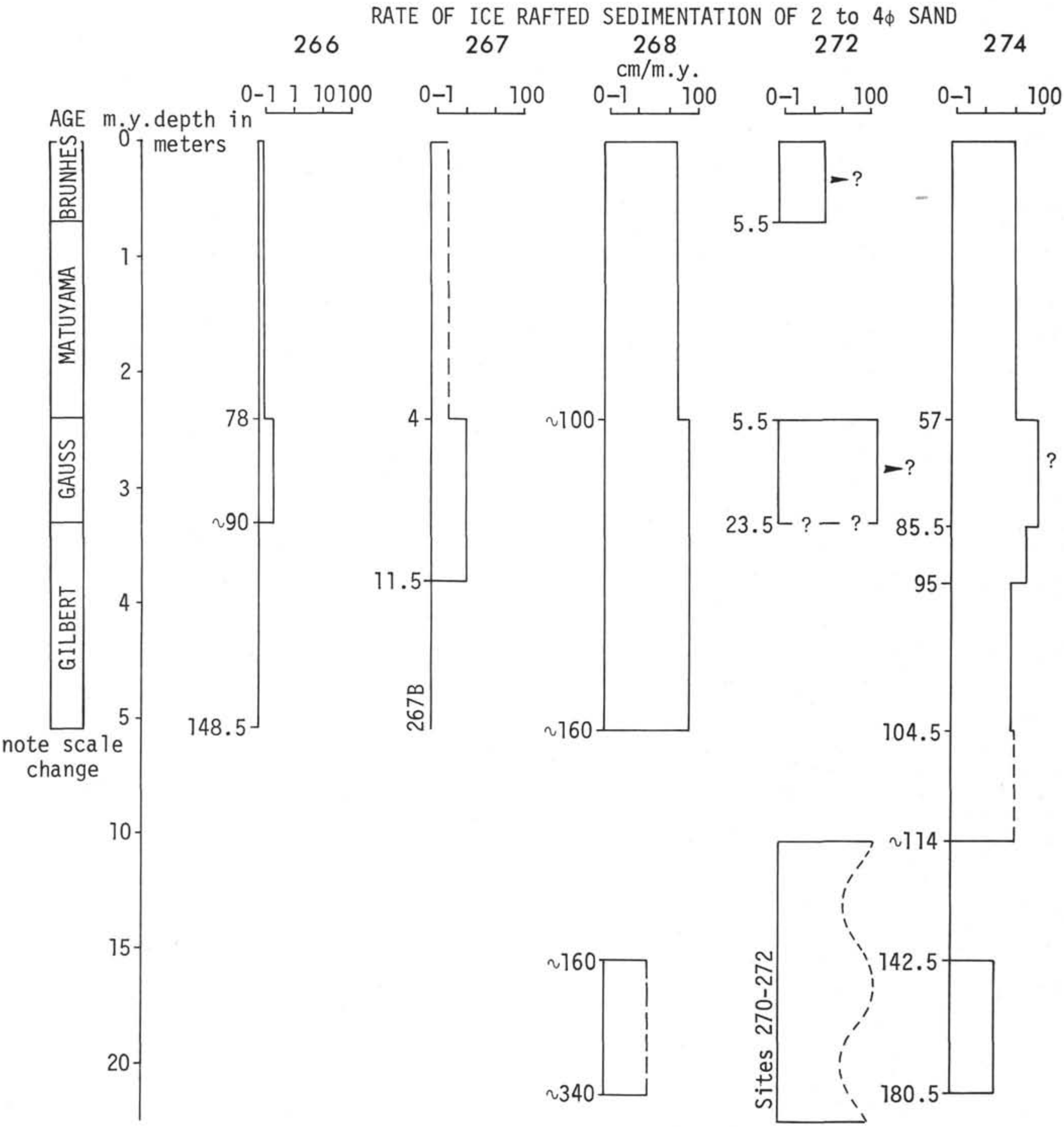

Figure 16. *Rates of accumulation of ice rafted 2 to 4Φ sand, in cm/m.y. Based on core thicknesses, abundance of sand (Table 4), and available biostratigraphic data. The biostratigraphic summary shown in Figure 3 of Chapter 1 (Introduction) has been used, with the following exceptions: Site 266: the assignment of the base of the Gauss is speculative. Site 267: dating of Core 1A (4-13 m) as Gauss disconformable on upper Gilbert is speculative, partly based on Radiolaria, and silicoflagellates (Ciesielski, personal communication). Hole 272: recognition of Brunhes part of sequence based on lithologic correlation with the cores of Fillon (1972) (see Barrett, Chapter 22). Note the Brunhes thickness is very uncertain. Hole 274: Position of top of Gauss uncertain; it may be lower than shown, in which case the Gauss might not be represented by recovered core. Detailed dating of Gilbert based mainly on silicoflagellates (Ciesielski, personal communication). Base of the upper Miocene may have been picked too low, so that the higher upper Miocene sedimentation rate may also apply to the topmost middle Miocene.*

TABLE 6
Electron Microprobe Analyses of Micronodules

Sample (Interval in cm)	Mn	Fe	Ti	Ca	Si	Mg	Ni	Cu	Al	Total Accounted for
	Percent Weights of Elements Expressed as Oxides									
274-10-6	29.6	1.9	0.7	1.9	29.0	3.2	n.d.[a]	n.d.	n.d.	66.2
and	26.4	1.4	1.1	0.6	22.1	2.4	n.d.	n.d.	n.d.	53.9
274-11-2	29.2	1.5	1.0	0.7	18.4	2.0	n.d.	n.d.	n.d.	52.7
	30.9	1.9	1.2	0.9	10.3	2.1	n.d.	n.d.	n.d.	47.2
	28.4	2.3	1.0	0.6	19.0	1.1	n.d.	n.d.	n.d.	52.4
	28.2	2.0	1.2	0.9	26.9	1.4	n.d.	n.d.	n.d.	60.6
266-11-6	59.4	0.5	0.4	0.9	3.3	3.0	0.1	0.4	n.d.	68.1
	62.9	0.3	0.6	1.0	1.0	3.1	0.2	0.6	n.d.	
272-2-2	0.15	0.9	1.1	0.4	70.5	0.8	n.d.	n.d.	n.d.	85.5
268-2-1	0.04	23.9	0.1	0.1	49.5	3.6	0.00	0.03	n.d.	77.3

[a]n.d. = element not determined after initial scan suggested very low concentration.

Site 268 were not recovered and this part of the section must be quite thin at this site. So little sand was found in the Miocene at Sites 267 and 266 that rate calculations are meaningless.

Fillon (1972) found abundant ice-rafted sand in Gauss and early Matuyama sediments in the Ross Sea and the area to the north around Site 274. Abundances were much lower in the late Matuyama, and intermediate amounts were found in Brunhes sediments. A correlation of Site 274 with Fillon's data suggests that the middle of Core 3 is mid-Matuyama. Note that the ice-rafted debris in the lower part of Core 2 and the upper part of core 3 (i.e., upper Matuyama by this correlation) has a high coarse- to fine-sand ratio.

The rate of ice-rafted sedimentation is closely related to distance offshore. The highest rates occur at Sites 274 and 268 on the continental rise and fall off rapidly northwards through Sites 267 and 266.

Rates at Site 269 are difficult to determine because of rapid turbidite sedimentation, but are comparable with those at Site 266. This may indicate that the rate of supply is dependent on proximity to a major source of bergs. Sites 266 and 268 lie a little way downcurrent from the Shackleton Ice Shelf; there is no major source of bergs immediately to the west of Site 269. Site 274 would be fed by Ross Ice Shelf bergs. If this interpretation is correct, it negates Warnke's (1970) suggestion that bergs depositing sediment travel great distances in the circumpolar current.

Rates will also depend on the preferred paths of icebergs, controlled by pack ice distribution and storm tracks. The effect of this on local variations in the rate of ice-rafted sedimentation is difficult to evaluate, but it seems inadequate to explain an overall very low rate of ice-rafting for tens of millions of years.

DETRITAL PETROLOGY

Introduction

This summary of the detrital sand petrology at Sites 267, 268, 269, and 274 is based on the following data:

1) Binocular microscope examination of about 120 sand fraction samples.

2) Petrologic microscope examination of about 20 grain mounts of sand fraction samples.

3) Petrologic microscope examination of nine thin-sectioned light mineral grain mounts in the size range 2.5-4ϕ (Table 7).

4) Ten heavy mineral separations, size range 2.5-4ϕ, separated with tetrabromoethane (Table 8).

5) About 20 thin sections of impregnated or lithified sediments.

6) Incidental data from shipboard smear slide descriptions by Ford (Site 267), Kemp (Site 268), and Barrett (Site 269).

Our data are generally consistent with those given by Barrett (Characteristics of Pebbles, this volume) for pebble lithology, and by Payne and Conolly (1972) for turbidite sands on the Wilkes Abyssal Plain.

Sand-size sediment at the sites investigated is probably transported in three ways: (a) ice rafting, active at all sites, but least important at Site 269; (b) transport by turbidity currents, especially at Site 269; (c) transport by bottom currents, especially at Site 268.

Sand Petrology

Turbidites from Site 274 show a strong influence of the Victoria Land basalts. The plagioclase to potassium feldspar ratio is higher than in the Wilkes Land sector (Table 7; Cook et al., X-Ray Mineralogy, this volume) and pyroxene is the dominant heavy mineral. In contrast, the only ice-rafted sample studied in detail was rich in hornblende, biotite, and opaques, and relatively poor in pyroxenes and garnet. This lithology is consistent with the lithology of the ice-rafted pebbles found at this site (Barrett, Characteristics of Pebbles, this volume). The quartz: feldspar ratio in the ice-rafted sands from Site 274 is very variable.

Site 269 has also received some sediment from a basaltic source. Pyroxene is the dominant heavy mineral, but hornblende and garnet are (as at Site 268) also present in quantity. The X-ray diffraction data of Cook et al. (this volume) show plagioclase to potassium feldspar ratios similar to those of Site 274, although our limited data do not confirm this.

Garnet, hornblende, and opaque minerals are the principal heavy minerals at Site 268, consistent with the ice-rafted lithologies. Cook et al. found subequal amounts of potassium feldspar and plagioclase.

TABLE 7
Light Mineral Petrology of Selected Samples From Sites 268, 269, and 274 (in percent)

Sample (Interval in cm)	Quartz: Single Crystal	Quartz: Micro-crystalline	Quartz: Polycrys-talline	Feldspar: K-Feldspar	Feldspar: Plagioclase	Feldspar: Altered	Rock Fragments	Micas	Calcite	Unknown	Sedimentation Process
268-2-2, 109-126	50.9	–	17.0	6.6	17.9	3.8	3.8	–	–	–	TU
268-5-2, 53-59	64.6	0.9	6.0	4.3	8.6	6.0	6.0	–	–	3.4	TU
269-1-6, 41-52	62.0	1.0	16.0	6.0	1.0	7.0	3.0	–	–	4.0	TU
269-3-3, 15-20	50.0	6.3	23.2	4.5	7.1	2.7	2.7	–	0.9	2.7	TU
269A-8-2, 84-117	50.9	1.9	23.6	5.7	1.9	3.8	1.9	–	–	1.0	TU
274-12-5, 100-6-50	38.9	1.1	18.9	3.3	4.5	15.6	12.2	–	–	5.6	IR
274-16-2, 130-145	46.1	–	8.9	4.0	9.8	6.9	11.8	1.0	4.9	6.9	TU
274-18-1, 120-122	54.5	1.8	13.6	6.7	5.5	5.5	6.7	0.9	1.8	3.6	TU
174-18-2, 20-22	57.4	0.9	10.2	5.6	10.2	7.4	3.7	–	1.9	2.8	TU

Note: TU = turbidity current; IR = ice-rafting. Light mineral 2-4ϕ fraction impregnated in epoxy resin and thin sectioned. At least 100 grains counted.

TABLE 8
Heavy Mineral Petrology of Selected Samples From Sites 268, 269, and 274 (in percent)

Sample (Interval in cm)	Garnet	Olivine	Green Hornblende	Brown Hornblende	Clinopyroxene	Hypersthene	Enstatite	Zoisite	Epidote	Chlorite	Biotite	Rock Fragments	Altered Grains	Opaques	Heavy Minerals	Sedimentation Process
268-2-2, 119-125	17.2	0.7	10.4	1.5	1.5	–	–	1.1	1.9	3.7	3.0	–	7.8	49.3	5.8	TU
268-5-2, 53-59	6.8	–	23.5	2.2	14.2	0.6	1.9	0.6	2.6	12.6	8.4	–	5.5	15.8	3.2	TU
269-1-6, 41-52	14.3	0.4	24.2	2.6	25.3	0.4	5.6	1.1	0.4	3.0	1.5	–	2.6	11.3	2.3	TU
269A-8-2, 84-87 & 113-117	12.5	–	12.5	–	38.7	1.2	6.4	2.5	0.4	1.7	0.4	–	3.0	11.2	3.1	TU
274-12-5 & 6	2.2	4.5	21.0	1.9	9.0	–	1.5	3.4	0.4	1.1	11.2	1.9	13.9	20.6	2.4	IR
274-18-1, 120-122	2.4	–	6.3	–	41.1	0.4	6.7	2.8	1.2	2.8	1.6	0.4	13.4	7.9	3.4	TU
274-18-1, 145-147	3.3	2.9	8.3	0.4	52.9	–	5.0	4.1	0.4	0.8	1.7	0.4	8.7	5.4	3.2	TU
274-18-2, 20-22	3.0	0.4	9.8	0.4	46.8	1.5	4.2	1.5	0.4	1.9	3.4	1.5	10.2	8.3	5.2	TU
274-18-2, 80-82	2.5	2.5	9.3	0.4	38.6	1.7	9.8	2.1	0.8	4.7	1.7	–	8.5	6.8	4.5	TU
274-18-2, 110-112	4.1	0.8	11.0	2.0	41.9	0.8	8.1	–	0.4	2.4	1.6	0.4	10.6	8.1	3.7	TU

Note: TU = turbidity current; IR = ice-rafting. About 300 grains counted in 2½ – 4ϕ size range.

Magnetite is very common in the upper part of the hole, where mafic plutonic rocks make up about 10% of the pebbles. Well-rounded quartz grains are common and correspond to those found in pebbles of medium- to fine-grain sandstone at this site (Barrett, Characteristics of Pebbles, this volume). Similar quartz grains are found at Site 267 (where the concentration of sand is insufficient for heavy mineral analysis). Our heavy mineral data in this sector differ from those of Payne and Conolly (1972) in that we find more garnet and less biotite than they do.

Clay Mineralogy

Clay mineral abundances have been replotted in Figure 17, with mica normalized to a value of 1.0, from the $<2\mu$ X-ray diffraction data reported by Cook et al. (X-Ray Mineralogy, this volume).

Kaolinite is found in the Pliocene-Quaternary of all three sites, but except for the upper Miocene at Site 274, is absent in older sediments. The kaolinite is presumably detrital from kaolinite-bearing rocks on the Antarctic continent. Terrigenous sequences (such as the Beacon Group) are frequently rich in kaolinite, although Barrett (1966) did not detect its presence in Beacon rocks that he examined.

Montmorillonite contents are highest in the lower part (Oligocene to early Miocene) of Site 269 (20%-30%; 0.7-3.0 normalized to mica = 1); in the upper part of the section, they decrease to 9%-15% (0.3-0.6 normalized to mica). Montmorillonite is abundant at Site 274, especially in the lower Pliocene and Miocene parts of the section (0.9-1.3 normalized to mica). Above and below this the normalized content ranges from 0.3 to 0.7, except for a montmorillonite-rich sample near the base of the hole. At Site 268, montmorillonite contents are low (0-0.3 normalized to mica) and show no general trends. There appears to be no relationship between the abundances of montmorillonite and volcanic ash seen in smear slides (Figure 17) (although operator variance might be the reason for this); but there is a broad correlation between the abundance of pyroxene of basaltic origin and the montmorillonite content. The montmorillonite is presumably detrital from the basalts and dolerites overlying the Beacon Group.

The first appearance of kaolinite in the latest Miocene indicates the time that the basaltic cover was breached and significant erosion of the Beacon Group occurred. The high montmorillonite content of the Miocene at Site 274 suggests rapid erosion of the basalts at that time; whereas at Site 269, maximum erosion appears to have taken place in late Oligocene times, and by the Miocene there was substantial dilution by erosion of other rocks (not Beacon, since kaolinite is lacking). The montmorillonite at Site 268 could perhaps have been supplied from volcanic rocks within the Beacon Group, or from ultramafic and mafic intrusions (cf. pebble data, Barrett, this volume); but the lack of Miocene or earlier kaolinite at both Sites 268 and 269 suggests that the Beacon was not substantially eroded before the Pliocene.

These data can be interpreted in several ways. We do not know how drainage basin areas have been modified since the middle Tertiary. Was there Tertiary uplift of the Transantarctic mountains? How much are the Miocene data for 268 modified by transport of clays by bottom currents? Much more detailed analysis is needed to resolve these problems.

FERROMANGANESE MICRONODULES

Distribution

Manganese nodules or micronodules were found in several cores from Leg 28. Macronodules were recognizable in split cores; micronodules were identified either in smear slides or in sieved sand fractions of samples.

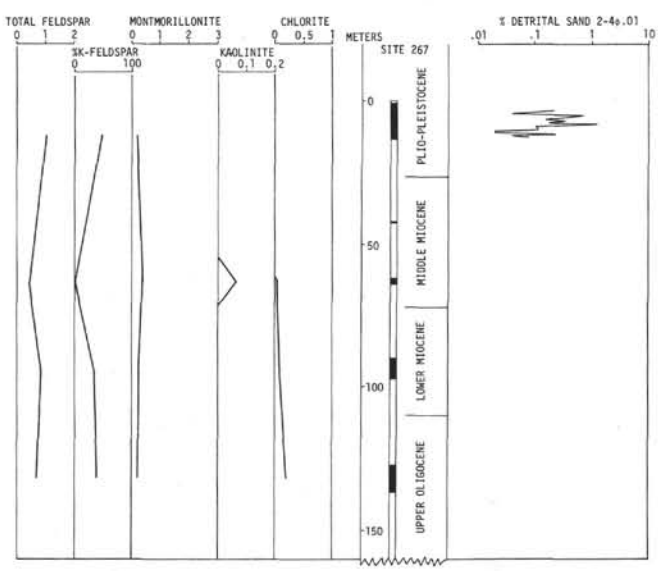

Figure 17. *Variations in petrology with depth at Sites 267, 268, 269, and 274. Note that vertical scale is different for Site 269. The percent detrital sand (Table 4) is believed to represent ice-rafted sediment in most cases. Montmorillonite, kaolinite, and chlorite values from the less than 2 M X-ray diffraction data of Zemmels (Chapter 00), normalized to mica = 1.0. Total feldspar, and percentage of feldspar that is K feldspar, based on bulk X-ray diffraction analysis by Zemmels, normalized to quartz = 1.0. Percent cristobalite based on bulk X-ray diffraction data. Note that adjacent data points have been joined purely to facilitate reading of the graph. No geologic predictions are intended. Presence of chert based on visual core description. Presence of volcanic glass (generally in trace amounts) based on smear slide identifications. Note the probability of operator variance in the recognition of volcanic glass.*

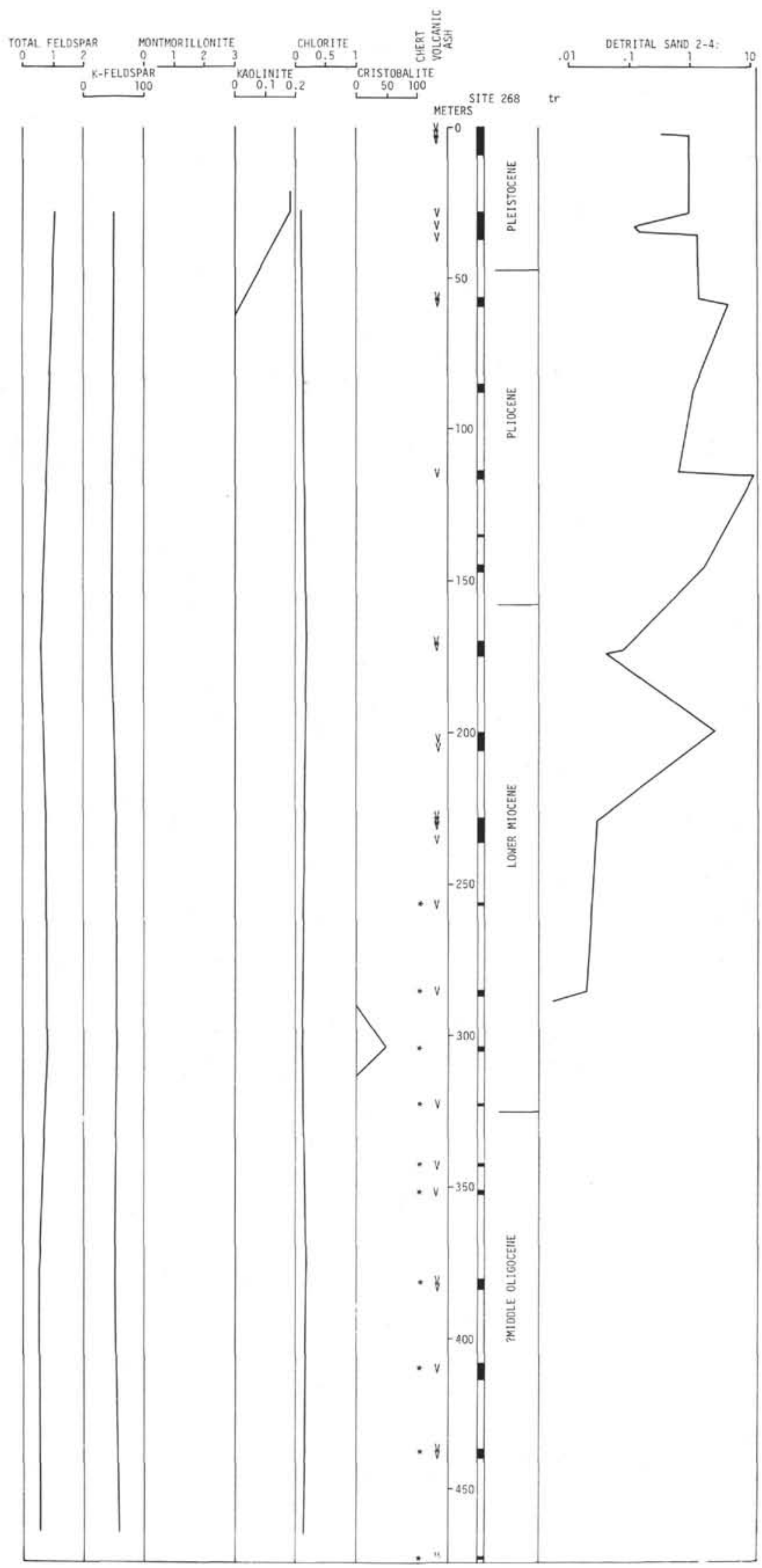

Figure 17. *(Continued).*

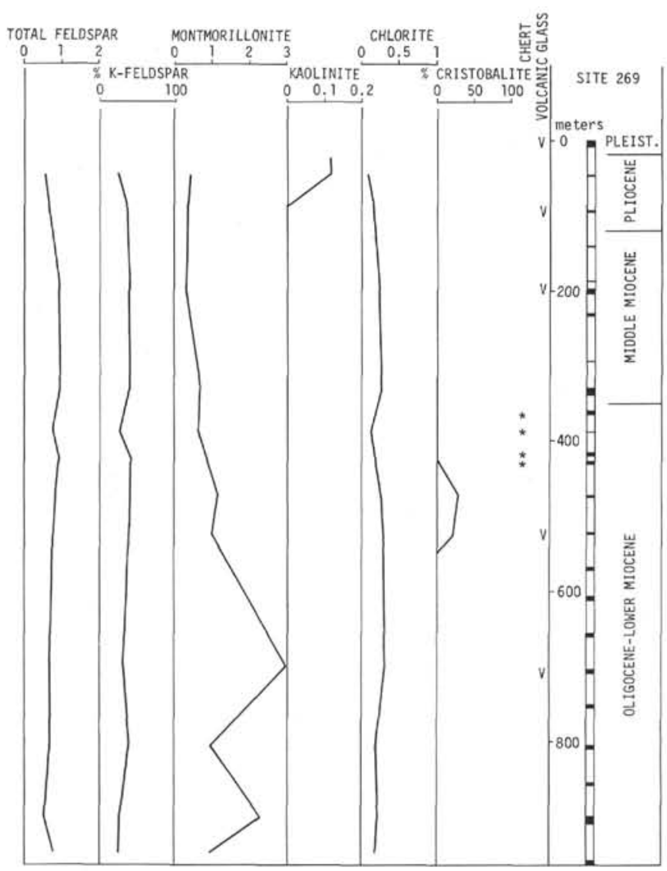

Figure 17. *(Continued).*

In the upper Miocene and lower Pliocene section of Site 274, from Core 10, Section 5 through Core 12, Section 6, manganese nodules are common. They are up to 2 cm in diameter and have a characteristic lumpy surface. Manganese-coated pebbles or clusters of pebbles are also common; coatings up to 2.7 mm thick were seen. Core logs suggest a 1 cm or larger manganese nodule per meter of core.

The only other site with macronodules was 267, where a cluster of pebbles with manganese oxide coatings 200μ-600μ thick occurs in Sample 1A-6, 10-13 cm. This section is probably of lower Pliocene age.

Brown micronodules in the 63μ-250μ size range have been found in several cores (Table 5). They are of two types: (a) dark, rough nodules with a matte surface very similar in appearance to the macronodules; (b) lighter colored micronodules, with a smooth shiny surface.

The dark rough nodules are found in the upper Miocene-lower Pliocene sequence at Site 274 which contains macronodules and are also common in a section of similar age in Cores 10 and 11 at Site 266. Dark, rough, Pliocene micronodules are found at Sites 266 and 267.

Smooth, light-colored micronodules are restricted to Plio-Pleistocene sediments at Sites 268 and 272. Fillon (1972) recognized apparently similar nodules in lower Pleistocene Ross Sea sediments in piston cores.

Chemical Composition of Micronodules

The chemical compositions reported here have been determined by electron microprobe. In some cases, due

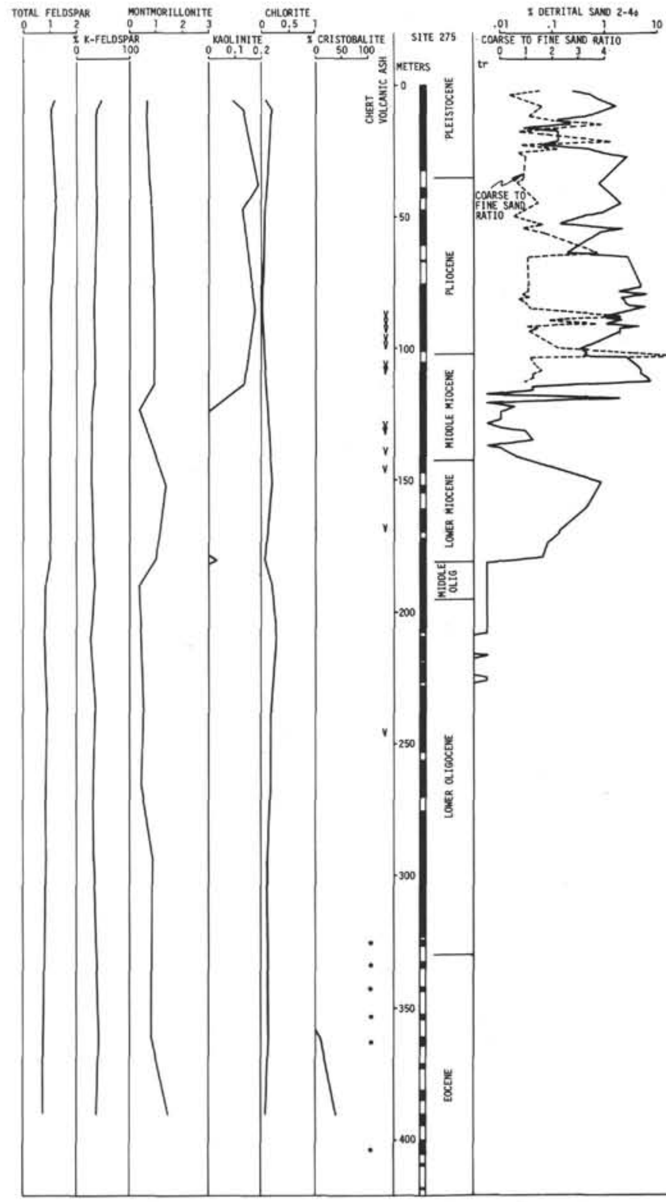

Figure 17. *(Continued).*

to the high friability of the nodules, considerable difficulty was encountered in preparing them for analysis. This problem, coupled with slight variations in elemental composition over nodule surfaces, has resulted in analyses which may only be regarded as semi-quantitative. Furthermore, most nodules probably contained substantial amounts of water which could not be detected on the microprobe.

Analyses in Table 6 are for micronodules from Sites 266, 268, 272, and 274. In some cases, it was necessary to prepare samples with micronodules hand-picked from several adjacent lengths of core.

The dark rough micronodules contain high concentrations of manganese. Silica contents are also high in the nodules analyzed from Site 274; spot checks on alumina content suggested it was low and similar to titania. This silica is probably dispersed biogenic opaline silica.

The two light, smooth nodules analyzed were low in manganese, but relatively high in silica, alumina, and iron. They may be some type of iron oxide aggregate or concentration associated with clays.

Discussion

The nodules and pebble coatings found in the Pliocene at Site 267 and the upper Miocene-lower Pliocene at Site 274 are associated with low rates of deposition. The pebble concentration at Site 267 was probably winnowed out by bottom currents, but there is no evidence from grain-size analyses (Figure 15) of winnowing at Site 274. Associated with the macronodules at these sites are micronodules of very similar physical appearance and limited analyses show close chemical similarities. Sequences with micronodules only also have low rates of sedimentation. There is no reason to suppose, however, that bottom currents are necessarily responsible.

Grains and aggregates of iron oxides are not uncommon in deep-sea sediments (see, for example, Cronan, 1973). The reason for their high concentration at certain levels at Sites 268 and 272 is not apparent.

CHERTS

Distribution

Porcellaneous cherts were found at Sites 268, 269, 272, and 274, in strata of Miocene and Oligocene age. All appear to result from cherty lithification of normal mudstone lithologies in sequences containing siliceous microfossils.

At Site 268, cherts occur from Core 11 (256 m) downward. No trends with depth were detected. Cherts are recovered as short blocks, suggesting original pebble-sized nodules or thin beds. They interbed with mudstones of varying colors and bedding structures. Most of the mudstones contain up to 5% diatoms and Radiolaria. The cherts appear to be lithified equivalents of the mudstones: all variants of the mudstones, including those with silt laminae, are represented by cherts. All degrees of lithification, from mudstone through porcellaneous chert, are present. The age of the sequence at Site 268 is probably middle Oligocene to early Miocene.

The occurrence of chert at Site 269 is almost identical to that at Site 268. Cherts are found in Cores 10 through 2A (359.5-435.5 m), of early Miocene age. Some cherty fine sandstones are found. Interbedded mudstones usually contain siliceous biogenic material. The section below the chert sequence appears to contain calcareous rather than siliceous microfossils, and there are carbonate cemented sandstone beds.

Chertified claystone occurs in blocks up to 20 cm long at Site 272, Cores 39-44 (365-422 m), of middle Miocene age. As at other sites, the cherts appear to be of lithified claystone or mudstone lithologies. Biogenic silica is very rare in the sediments associated with cherts; overlying cores contain a few diatoms and Radiolaria.

At Site 274, cherts occur from Core 35 to 39 (323-380 m), but are absent below this down to basalt basement at 408.5 meters, with the exception of a minor chertified mudstone in Core 43, Section 2. This cherty sequence is of Eocene age. Claystones interbedded with the cherts contain only trace quantities of biogenic silica, as do those in the section below the cherty sequence. Above the chert sequence is a thick section of diatomite and diatom ooze.

Observations in Hand Specimen

The hardness of chert is revealed in two ways in hand specimen. Conchoidal fractures are developed only in chert and not in associated mudstone. The diameter of the sediment core decreases with increasing hardness. There are no dense vitreous cherts composed of recrystallized quartz. The most indurated cherts described here have a hardness of only about 4 on Moh's scale.

Observations in Thin Sections

Cherts from Sites 268 and 269 are indistinguishable in thin section from sections of impregnated mud from the same cores. Distinct diagenetic silica is not recognizable. Under crossed polars there is usually a gross extinction in the groundmass parallel to bedding. In muds this is due to parallel orientation of clay minerals, but could be enhanced by silica in cherts. In one chert thin section (268-13-1, 100-150 cm), the specimen is divided into many different fields of parallel extraction, with sharp irregular boundaries between the fields, suggestive of diagenetic mineral growth. Fragments of diatoms and Radiolaria are preserved in all the cherts examined, without showing any visible solution effects, and in some sections are very abundant. Radiolaria with a coating of an opaque mineral (?pyrite), similar to those in unlithified sediments, are found in some cherts from Site 268.

In cherts from Site 272, Radiolaria have not been seen, but diatom fragments are very common, both in the cherts and in immediately adjacent mudstones.

Examination with Scanning Electron Microscope

A few chert samples have been briefly examined under the SEM. No clear evidence has been seen of solution of biogenic siliceous fragments. No growth of nodular cristobalite as reported by Heath and Moberley (1971) has been seen, but the coarseness of detrital quartz grains in the cherts may obscure such features.

X-Ray Diffraction

The main silica phases prrsent have been identified by X-ray diffraction. Samples were crushed with a stainless steel morta and pestle and then ground to powder by a 20-min treatment in a tungsten carbide ball mill. Random mounts were made in an aluminum holder. The samples were run on a Phillips PW4620 X-ray diffractometer. Instrument settings were: 40 kv; 20 mA; time constant 4 sec; 400 cps; chart speed 20 mm/min; scanning speed $1°2\theta$ per min; scanning range 15° to 28° 2θ.

At Site 268, quartz gives prominent peaks in all samples. In addition, almost all cherts have a broad peak between 21.5° and 22. 2θ which is identified as poorly crystallized cristobalite (cf. Heath and Moberly, 1971), otherwise known as lussatite (von Rad and Rösch, 1972). This peak is sharpest, indicating the greatest ordering of the cristobalite, in the hardest cherts (G and H, Figure 18). Only one chert (J, Figure 18) has no detectable cristobalite peak: in thin section this chert is seen to consist of a nodule (?load cast) of well-sorted 20μ quartz silt, apparently cemented with silica (the cement is difficult to resolve). Quartz-dominated cherts like this are very rare in Leg 28 sites. Cristobalite is found in mudstones within 1 cm of chert beds or nodules, but is not found in mudstones more than 1 cm from chert (e.g., C and I, Figure 18).

At Sites 272 and 274, the cristobalite peak is much more prominent, perhaps in part because of the smaller detrital quartz content of the sediments. It occurs not only in cherts, but also in indurated mudstones both associated with chert (e.g., Figure 18: N, 2 cm from chert; P, 1 cm from chert) and also from lengths of core in which chert appears absent (e.g., T and Q, Figure 18). It is, however, not found in unlithified diatom clay ooze from the lower part of Site 274 (Figure 18: U from 274-33-6).

Discussion

The cherts from Leg 28 differ from most cherts recovered by DSDP in being developed in terrigenous sediments. Detrital quartz and clay are a hinderance in investigating these cherts.

The diagenetic sequence inferred from these cherts is similar to that found by Heath and Moberly (1971) and von Rad and Rösch (1972). Disordered cristobalite develops in sediments inferred to originally contain biogenic opaline silica; and the cristobalite becomes more ordered with time. The final stage of inversion of cristobalite to quartz has not been observed in Leg 28 cherts. There is no evidence at all of possible volcanic source materials for the silica. But neither do the siliceous skeletons preserved in the chert appear corroded.

The clearest evidence of a biogenic origin for the silica in the cristobalite is the restriction of chert at Site 269 to the deepest part of the section with common siliceous microfossils. Chert is absent from the underlying sequence which contains coccoliths and foraminifera. The abrupt reduction of siliceous microfossil abundances at about the level where chert first appears in Hole 274 may also be evidence of a biogenic source.

Smear slides of mudstones associated with cherts show abundant fragments of diatoms, apparently ranging in size down to the limits of resolution (say, 5μ). In thin sections, it is difficult to resolve fragments of less than 20μ. It is possible that the main source of silica is finely comminuted diatom debris. Fragments in the few-micron size range would tend to dissolve readily, even if larger fragments showed little sign of corrosion.

DISCUSSION AND SYNTHESIS

Ice-Rafting

Source

Our petrologic data and that of Barrett (Characteristics of Pebbles, this volume) suggest that the source of ice-rafted debris for Site 274 was the Ross Sea and to a lesser extent Victoria Land, while that at Sites 267 and 268 came from elsewhere, perhaps the Shackleton Ice Shelf. The very low percentage of ice-rafted debris at Site 269 is partly an effect of the high sedimentation rate, but primarily reflects a lack of sediment-bearing icebergs.

Factors Controlling Rates of Ice-Rafted Sedimentation

Four main factors appear to control the rate of ice-rafted sedimentation (Carey and Ahmad, 1961; Warnke, 1970; Fillon, 1972; Anderson, 1972): (1) rate of continental erosion; (2) thermal structure of glaciers or ice shelves, and hence both their erosional and melting behavior; (3) size of ice shelves; (4) sea temperatures.

How these factors affect sedimentation rate is disputed. A dry-base ice shelf may result in basal freezing, and less sediment will be deposited beneath or close to the ice shelf. The larger a wet-base ice shelf is, the more sediment will be deposited beneath it, and the less will move out to sea in bergs.

Cold bottom water generated by a large dry-base ice shelf may form a powerful deep-water bottom current. However, evidence of bottom currents in cores may result from other causes; for example, reduced ice-rafted and biogenic sedimentation or bottom currents resulting from bathymetric constrictions of deep-water movement. We have definite evidence of bottom currents in the Miocene at Site 268 and in the early Pliocene(?) at Site 267. Manganese nodule accumulations may reflect bottom-current activity (Goodell et al., 1971), but this cannot be demonstrated from our data.

Since glaciation was initiated at least as early as upper Oligocene, by late Miocene time major variations in the rate of continental erosion are unlikely to have resulted from variations in the resistance of source rocks, especially from such a large source area. Barrett's pebble data (Characteristics of Pebbles, this volume) is consistent with this interpretation. However, since the X-ray diffraction data (Cook et al., X-Ray Mineralogy, this volume) suggests little erosion of the Beacon Group until the early Pliocene, there may be some small long-term trends in the rates of erosion.

We can say little about the detailed history of Antarctic ice cover because of intermittent core recovery and poor biostratigraphy. Our dating is good to perhaps one million years; fluctuations in ice conditions are likely to be on the order of tens to hundreds of thousands of years.

Despite these limitations, we can roughly characterize the dominant ice-shelf conditions during each of the last four major magnetic epochs, on the basis of variations in the type and rate of ice-rafted sediment accumulation.

Throughout the Brunhes-Matuyama (biostratigraphy inadequate to subdivide), ice-rafted sediments are characterized by moderate rates of deposition at all sites, decreasing offshore, and with a low coarse to fine sand ratio at Site 274. During the (probable) upper Matuyama, Site 274 experienced a low sedimentation rate of ice-rafted material, with a high coarse to fine sand ratio. The (approximate) Gauss has universally higher rates of sedimentation. Because of limited recovery at Site 274, the coarse to fine sand ratio is un-

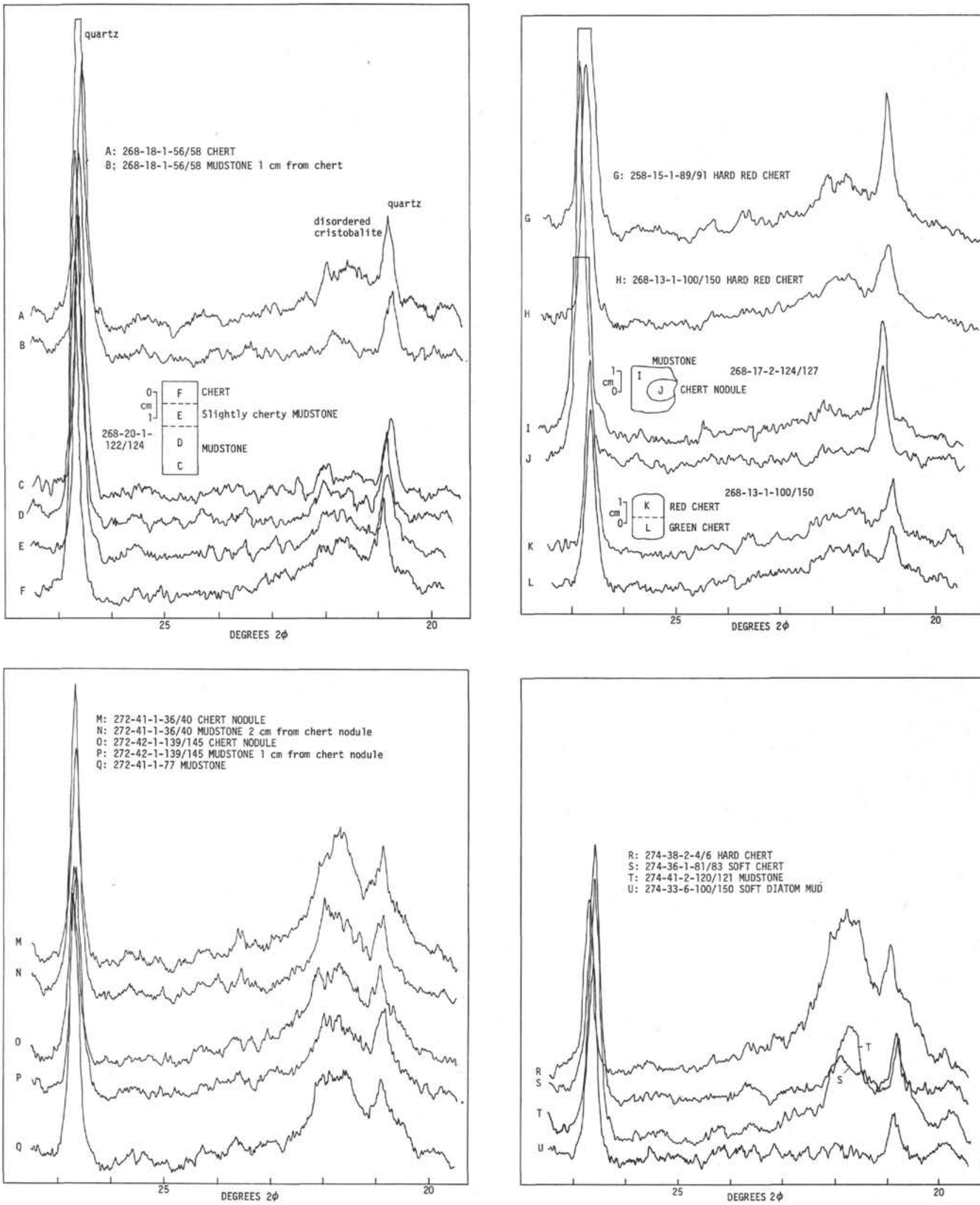

Figure 18. *X-ray diffractograms of cherts and mudstones from Sites 268, 272, and 274, showing development of disordered cristobalite in different lithologies.*

certain. During the (approximate) Gilbert, there were moderate to high rates of ice-rafted sedimentation at nearshore sites, but very low rates at offshore Sites 266 and 267. At Site 274, the coarse to fine sand ratio is high.

The data for the lower Matuyama and the whole of the Brunhes suggest that mostly wet-base ice-shelf conditions dominated, with the upper Matuyama interval most simply explained by an intensification of wet-base conditions. The universally higher rates in the (approximate) Gauss indicate that less material was being deposited further inshore than our sites, possibly due to the formation of a dry-base ice shelf. The Ross Sea unconformity might have formed at this time. In the (approximate) Gilbert, the rapid decrease in rates offshore suggests a resumption of wet-base ice-shelf conditions accompanied by rapid melting of icebergs. This would be in agreement with the warm water temperatures suggested by Ciesielski and Weaver (1973).

We must emphasize, however, that these suggestions are speculative.

Turbidity Currents

Initiation of Turbidity Currents

The shelf break around Antarctica is unusually deep and would have remained in quite deep water even during eustatic lowerings of sea level at glacial maxima. On most continental margins of the world, submarine canyons were eroded when sea level was lowered. Except off major deltas, most present-day and late Pleistocene turbidites appear to have been derived from submarine canyons heading in very shallow water. Only these canyons that have maintained their heads in shallow water during the Recent transgesssion actively funnel sand to deep water at the present time. Turbidity currents in such submarine canyons are probably initiated by rip currents during storms, and transport large amounts of sand.

There are few documented turbidity currents derived from mudflows or slides, other than on major deltas, or in areas of glaciomarine sedimentation. The Grand Banks Slump and turbidity current of 1929 was initiated in an area of major Pleistocene deposition from floating ice. Marlowe (1968) presents evidence that turbidites in Baffin Bay are generated by muddy slumps.

In turbidity currents generated by rip currents flowing over nearshore sandy sediments, even proximal sands will be relatively well sorted and free of mud. In contrast, a slump or mudflow will start off with very poor sorting and large amounts of mud. Lengthy travel will be needed for a well-sorted sand to separate out at the base of the turbidity current. Thus graded sands with a high content of mud will be expected from such slump-generated turbidity currents, in contrast to the well-sorted graded sands of rip current-generated turbidity currents.

Such muddy sands (and indeed, also a mudflow) are found at Site 268; the much better sorting of sands and silts at Site 269 probably results from the turbidity currents having traveled much further.

These ideas could be further evaluated by seeing if the canyons and valleys of the Antarctic continental slope resemble normal submarine canyons, or if they are closer to the slump scars characteristic of the area of the Grand Banks Slump, where the continental shelf break is also well below the depth of glacially lowered sea level.

Proximal-Distal Changes

Site 269 confirms the observations of Payne and Conolly (1972) on proximal to distal changes in turbidites in the south Indian Abyssal Plain. Sediments in the distal part of the plain consist of 60% turbidite clay and mud, 20% turbidite silt, 2% turbidite sand, and 18% mud of uncertain origin. Turbidite sands and coarse silts are increasingly common on the more proximal parts of the plain.

Continental Margin Progradation

Lithologic changes at Sites 268 and 269 are evidence of substantial progradation of the continental margin, which is also shown in seismic reflection profiles. At both sites there is a transition from more distal facies in the lower parts of holes to more proximal facies near surface.

At Site 267 there is evidence of bottom current activity throughout the late Cenozoic. In the Miocene strata of Site 268 laminated silts, probably indicating contour current activity, predominate and middle and upper Miocene sediments are thin or absent; but in the Plio-Pleistocene there is no evidence of contour currents. Instead, there are thicker turbidite silts and in the topmost core, sands and pebbly muds.

Likewise at Site 269 turbidite silts and clays dominate the lower part of the section and sands become increasingly important in the upper part of the hole.

These data could alternatively be interpreted as evidence of increased supply of sand and coarse silt, compared with fine silt and clay, from the Antarctic continent through the late Cenozoic. Such an interpretation is not consistent with evidence in the Ross Sea sector and is not a necessary hypothesis.

ACKNOWLEDGMENTS

Responsibilities for authorship are: detrital petrology and ferromanganese micronodules—C. D. Brisco and D. J. W. Piper; other sections—D. J. W. Piper.

Laboratory work was supported by Canadian NRC Grant No. A8390. R. MacKay assisted with electron microprobe analysis. X-ray diffractograms were produced at the Department of Geology, Memorial University, Newfoundland, through the courtesy of Roger Slatt. Romi von Borstel carried out some of the size analyses. We thank Roland von Huene for useful discussion and Peter Barrett for encouragement.

REFERENCES

Anderson, J. B., 1972. Nearshore glacial-marine deposition from modern sediments of the Weddell Sea: Nature Phys. Sci., v. 240, p. 189-192.

Barrett, P. J., 1966. Petrology of some Beacon rocks between the Axel Heiberg and Shackleton Glaciers, Queen Maud Range, Antarctica: J. Sediment. Petrol., v. 36, p. 794-805.

Bouma, A. H., 1972. Sedimentology of flysch deposits: Amsterdam and New York (Elsevier).

Bouma, A. H. and Hollister, C. D., 1973. Deep ocean basin sedimentation. *In* Middleton, G. V. and Bouma, A. H. (Eds.), Turbidites and deep water sedimentation, Pacific section SEPM: p. 79-118.

Carey, S. W. and Ahmad, N., 1961. Glacial marine sedimentation. *In* Raasch, G. O. (Ed.), Arctic Geol.: v. 2, p. 865-894.

Ciesielski, P. F. and Weaver, F. M., 1973. Southern ocean Pliocene paleotemperatures based on silicoflagellates from deep-sea cores: Antarctic J. U.S., v. 8, p. 295-297.

Cronan, D. S., 1973. Basal ferruginous sediments cored during Leg 16, Deep Sea Drilling Project. *In* van Andel, T. H., Heath, G. R., et al., Initial Reports of the Deep Sea Drilling Project, Volume 16: Washington (U.S. Government Printing Office), p. 601-604.

Field, M. E. and Pilkey, O. H., 1971. Deposition of deep sea sands: comparison of two areas of the Carolina continental rise: J. Sediment. Petrol., v. 41, p. 526-536.

Fillon, R. H., 1972. Late Cenozoic geology, paleo-oceanography and paleo-climatology of the Ross Sea, Antarctica: Ph.D. dissertation, University of Rhode Island.

Goodell, H. G., Meylan, M. A., and Grant, B., 1971. Ferromanganese deposits of the South Pacific Ocean, Drake Passage and Scotia Sea: Am. Geophys. Union Antarctic Res. Ser., v. 15, p. 93-168.

Heath, G. R. and Moberly, R., 1971. Cherts from the western Pacific: Leg 7, Deep Sea Drilling Project. *In* Winterer, E. L., et al., Initial Reports of the Deep Sea Drilling Project, Volume 7: Washington (U.S. Government Printing Office), p. 987.

Kelts, K. and Briegel, V., 1971. Sediment slides and turbidity current models from Swiss lakes: Internatl. sediment. congr. 8th, Heidelberg. (Abstracts)

Kennett, J. P. and Brunner, C. A., 1973. Antarctic late Cenozoic glaciation: evidence for initiation of ice rafting and inferred increased bottom water activity: Geol. Soc. Am. Bull., v. 84, p. 2043-2052.

Kuenen, P. H., 1966. Matrix of turbidites: experimental approach: Sedimentology, v. 7, p. 267-297.

Marlowe, J. I., 1968. Unconsolidated marine sediments in Baffin Bay: J. Sediment. Petrol., v. 38, p. 1065-1078.

Normark, W. R. and Piper, D. J. W., 1972. Sediments and growth pattern of Navy deep sea fan, San Clemente Basin, California borderland: J. Geol., v. 80, p. 198-223.

Payne, R. R. and Conolly, J. R., 1972. Turbidite sedimentation off the Antarctic Continent: Am. Geophys. Union Antarctic Res. Ser., v. 19, p. 349-364.

Piper, D. J. W., 1972a. Sediments of the middle Cambrian Burgess Shale, Canada: Lethaia, v. 5, p. 169-175.

_______, 1972b. Turbidite origin of some laminated mudstones: Geol. Mag., v. 109, p. 115-126.

_______, 1973. The sedimentology of silt turbidites from the Gulf of Alaska. *In* Kulm, L. D., von Huene, R., et al., Initial Reports of the Deep Sea Drilling Project, Volume 18: Washington (U.S. Government Printing Office), p. 847.

Selley, R. C., 1970. Studies of sequence in sediments using a simple mathematical device: Quart. J. Geol. Soc. London, v. 125, p. 557-581.

von Huene, R., Larson, E., and Crouch, J., 1973. Preliminary study of ice-rafted erratics as indicators of glacial advances in the Gulf of Alaska. *In* Kulm, L. D., von Huene, R., et al., Initial Reports of the Deep Sea Drilling Project, Volume 18: Washington (U.S. Government Printing Office), p. 835-842.

von Rad, U. and Rösch, H., 1972. Mineralogy and origin of clay minerals, silica and authigenic silicates in Leg XIV sediments. *In* Hayes, D. E., Pimm, A. C., et al., Initial Reports of the Deep Sea Drilling Project, Volume 14: Washington (U.S. Government printing Office), p. 727.

Warnke, D. A., 1970. Glacial erosion, ice rafting and glacial marine sediments: Antarctica and the Southern Ocean: Am. J. Sci., v. 269, p. 279-294.